

Research Activities 2013-2019

OUTLINE:

- Physics Analysis at CMS/LHC
- HDQM Tool for CMS Tracker
- HL-LHC : CBC2 Test Beams, Outer tracker sensor evaluation
- Radioactive source localization
- New UV sensor based on MWCNT
- Future Plans

Search for general gauge-mediated supersymmetry in final states with two photons and missing transverse momentum

A. Askew¹, A. Reinsvold Hall², M. Hildreth², A. Kyriakis³, T. McCauley²,
I. Topsis-Giotis³, G. Paspalaki³, A. Santra¹, M. Weinberg¹

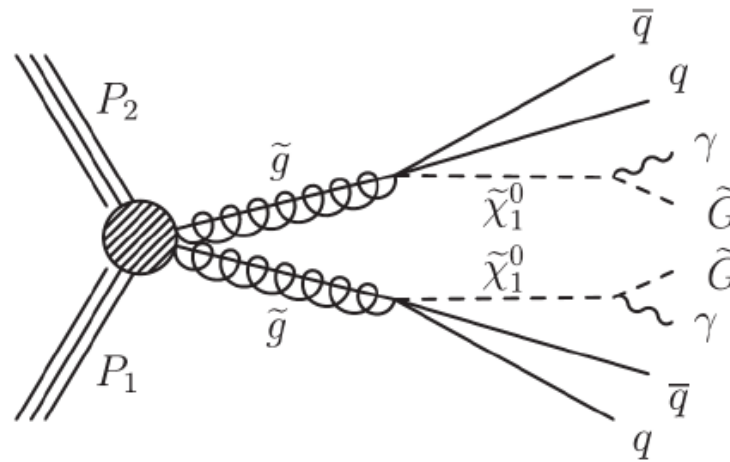
¹ Florida State University

² University of Notre Dame

³ National Center for Scientific Research Demokritos

INTRODUCTION

- Final states in pp collisions with high- E_T photons and significant E_T^{miss} emerge naturally from a variety of new physics scenarios, particularly in models of supersymmetry (SUSY) broken via gauge mediation and including a stable, weakly interacting lightest supersymmetric particle (LSP)
- Models with general gauge mediation (GGM) can have a wide range of features, but typically entail a gravitino LSP and a next-to-lightest supersymmetric particle (NLSP) commonly taken to be a neutralino or a stau.

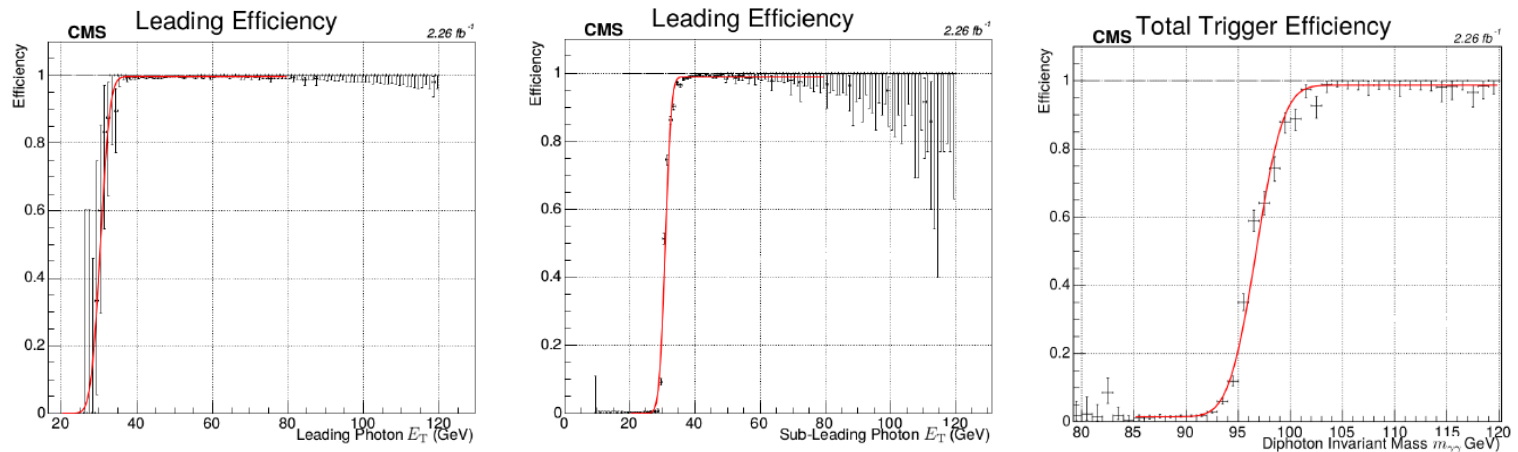


- Signature : Characteristic events with jets, two photons and large E_T^{miss}

Analysis Strategy

The first analysis for the T5gg channel used the data sample corresponds to an integrated luminosity of 2.32 fb^{-1} of pp collisions at $\sqrt{s} = 13 \text{ TeV}$ collected with the CMS/LHC in 2015.

Primary analysis trigger (ECAL Barrel region used, $|\eta| < 1.4442$):
HLT_Diphoton30_18_R9Id_OR_IsoCalId_AND_HE_R9Id_Mass95



HLT efficiency is calculated by a tag and probe method and is 98.6% for photon $P^T > 40 \text{ GeV}$

Trigger requires two photons passing the sub-leading filter and one photon passing the leading filter, so that the total efficiency $\epsilon_{\text{tot}} = \epsilon_{\text{lead,lead}} \times \epsilon_{\text{lead,sub}} \times \epsilon_{\text{sub,sub}}$

Offline Selection

Photons

- From PF photon Collection
- $P_T > 40\text{GeV}$
- $|\eta| < 1.4442$
- Passes medium photon ID
- Passes Pixel seed veto

Jets

- $P_T > 30\text{GeV}$
- $|\eta| < 2.4$
- Passes PF Loose ID
- Remove jets that overlap within $\Delta R < 0.4$ of a muon, electron, or a photon

Muons

- $P_T > 30\text{GeV}$
- $|\eta| < 1.4442$
- Passes medium muon ID
- Passes loose muon isolation

Electrons

- From PF photon collection
- $P_T > 40\text{GeV}$
- $|\eta| < 1.4442$
- Passes medium photon ID
- Fails pixel seed veto
- Remove electrons that overlap within $\Delta R < 0.4$ of a muon

$$E_T^{\text{miss}} > 100\text{ GeV}$$

Backgrounds

Quantum Chromodynamics (QCD) background:

- Most significant background due to huge QCD cross section
- Can have real photons in the final state or we can get electromagnetically-rich jet fragmentation mimicking the response of a photon
- E_T^{miss} comes from mis-measured hadronic activity.

Electroweak (EWK) background:

- Includes W and W + jet events
 - $W \rightarrow e\nu$ and the electron is misidentified as a photon
 - W + jet events, one of the jets fakes a photon
- Genuine E_t^{miss} from the neutrino

Other backgrounds-small and studied with Monte Carlo (MC):

- $Z \gamma\gamma \rightarrow \nu\nu\gamma\gamma$
- $W\gamma\gamma \rightarrow l\nu\gamma\gamma$
- $t\bar{t}b\gamma\gamma$

Estimated background events and systematics

Table 8.6: Estimation of total QCD background for $E_T^{\text{miss}} > 100$ GeV

E_T^{miss} range (GeV)	Background Prediction
100 – 110	1.85 ± 0.96
110 – 120	1.53 ± 0.63
120 – 140	0.97 ± 0.62
> 140	0.61 ± 2.15

Table 8.10: Systematic and Statistical Uncertainties from QCD Background Estimation

E_T^{miss} bin (GeV)	Systematic Uncertainty	Value
100 – 110	Di-EM p_T reweighting	15.11%
	Jet multiplicity reweighting	33.77%
	Shape difference between ee and ff	18.18%
	Statistical uncertainty of ee sample	30.81%
110 – 120	Di-EM p_T reweighting	16.60%
	Jet multiplicity reweighting	14.87%
	Shape difference between ee and ff	12.07%
	Statistical uncertainty of ee sample	33.33%
120 – 140	Di-EM p_T reweighting	33.31%
	Jet multiplicity reweighting	29.39%
	Shape difference between ee and ff	14.40%
	Statistical uncertainty of ee sample	41.75%
140 – <i>Inf</i>	Di-EM p_T reweighting	39.37%
	Jet multiplicity reweighting	20.34%
	Shape difference between ee and ff	150.36%
	Statistical uncertainty of ee sample	70.98%

Table 8.8: Estimation of the total EWK background for $E_T^{\text{miss}} > 100$ GeV

E_T^{miss} range (GeV)	Expected
100 – 110	0.41 ± 0.12
110 – 120	0.26 ± 0.09
120 – 140	0.54 ± 0.15
> 140	1.03 ± 0.25

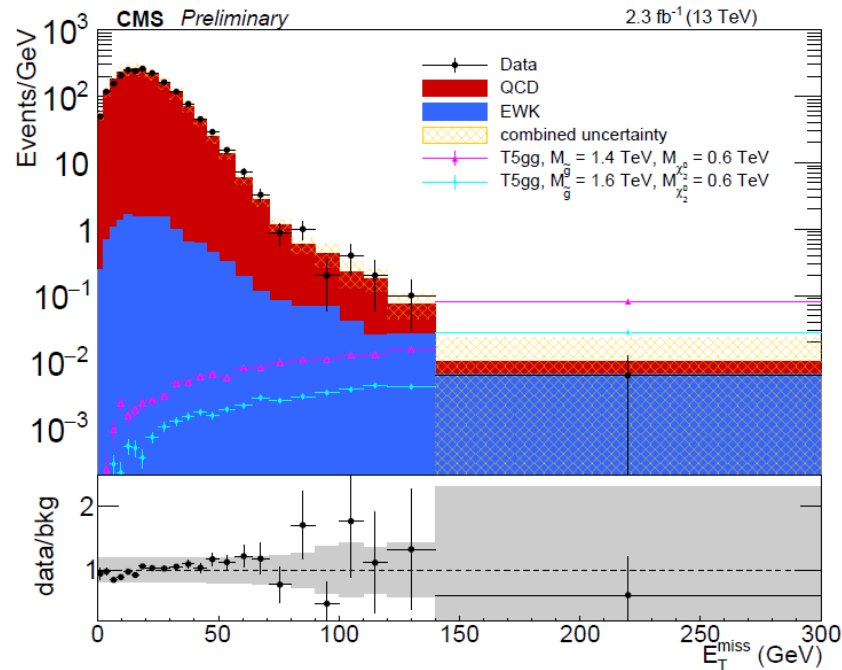
Table 8.11: Summary of systematic uncertainties included in the determination of the expected exclusion contours.

Systematic Uncertainty	[%]
Integrated luminosity	4.6
Photon Data/MC scale factor	2.4
Jet energy scale	0 - 23
Finite MC statistics	0 - 16
PDF error on cross section	13 - 22

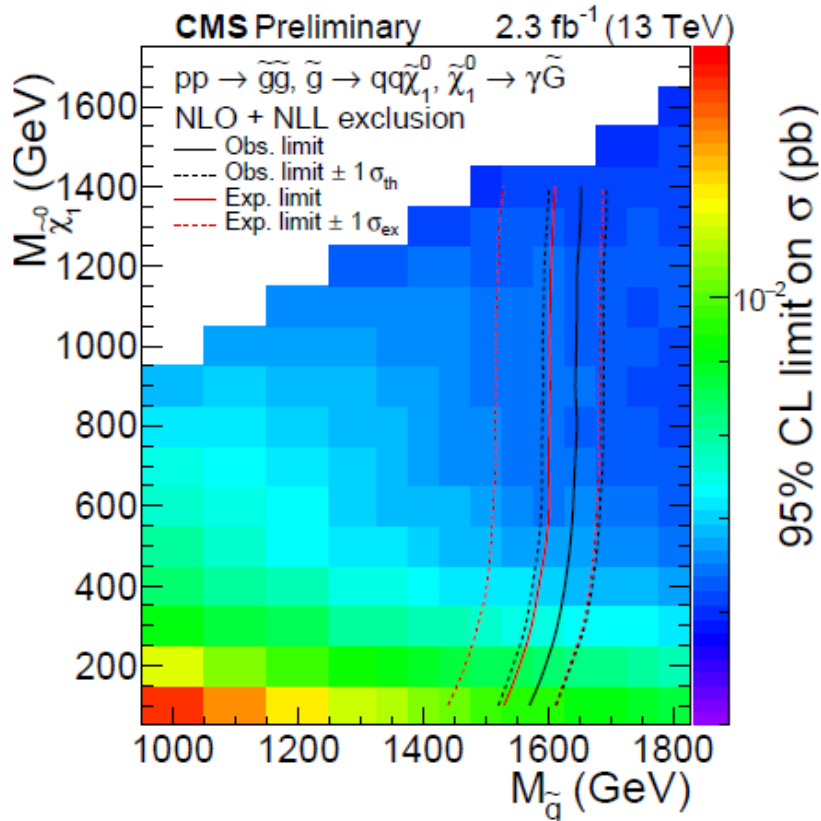
Estimated - Observed events for T5gg model at 2.3fb^{-1}

Table 8.9: Expected and observed events for $E_T^{\text{miss}} > 100 \text{ GeV}$

E_T^{miss} range (GeV)	Expected	Observed
100 – 110	2.26 ± 0.96	4
110 – 120	1.79 ± 0.64	2
120 – 140	1.51 ± 0.64	2
> 140	1.64 ± 2.16	1



Mass Limits for gluino using 2.9fb^{-1}



- An expected exclusion reach for the analysis was done using the modified frequentist CLs methods
- This is based on long-likelihood test statistic that compares the likelihood of the SM-only hypothesis to the likelihood of the presence of signal in addition to the SM conditions
- The likelihood function are based on the expected shape of the E_T^{miss} distribution for signal and background in four separate bins.
- For typical values of neutralino mass, we expect to exclude gluino masses out of 1.5 TeV, improving the reach of previous searches performed at center-of-mass energies of 8 TeV.

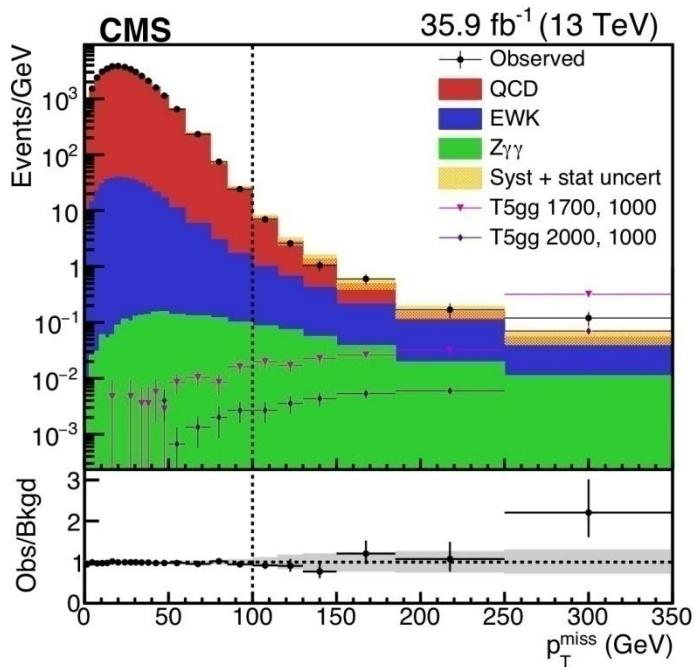
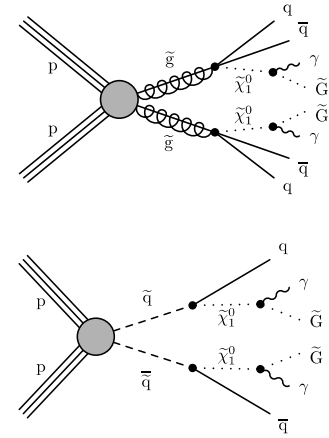
This work is part of Iasonas Topsis-Giotis's thesis successfully defended in 2017

Analysis for both T5gg and T6gg model with full 2016 data set

Simplified Models:

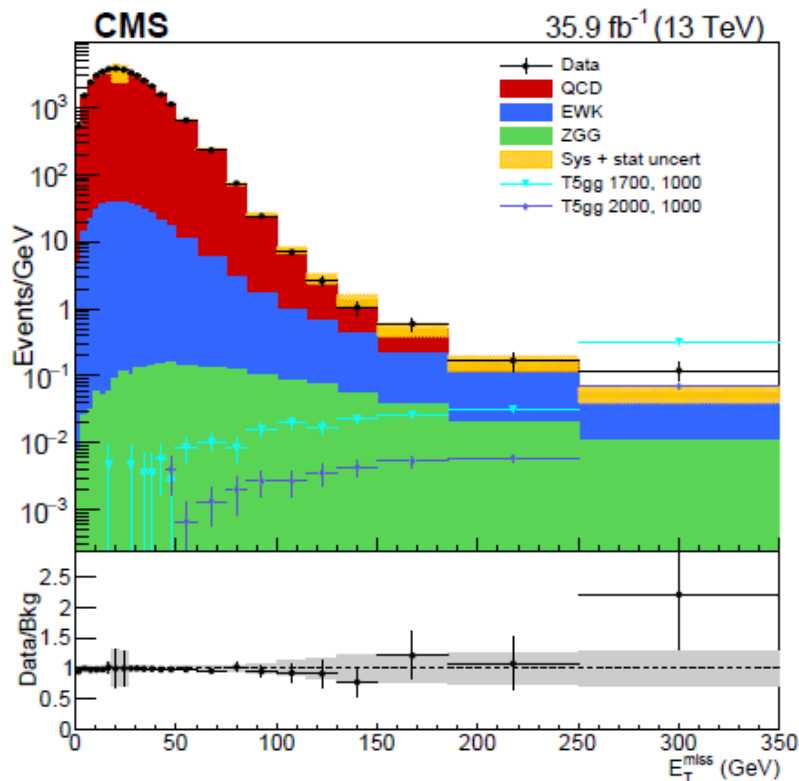
- strong production via gluinos/squarks
- **T5gg model**: gluino decays to a quark and a neutralino
- **T6gg model**: squark decays to a quark and a neutralino

In both cases we assume 100% branching fraction for neutralino decaying to a **gravitino and a photon**.



- background estimation for **QCD**, **EWK** and **Zγγ**
- Compare predicted number of events to observed in the **six signal bins**
- **signal region** : $p_T^{miss} > 100$ GeV
- observe an excess in the last bin
- taking all signal bins into account we observe a 2.4 standard deviation excess

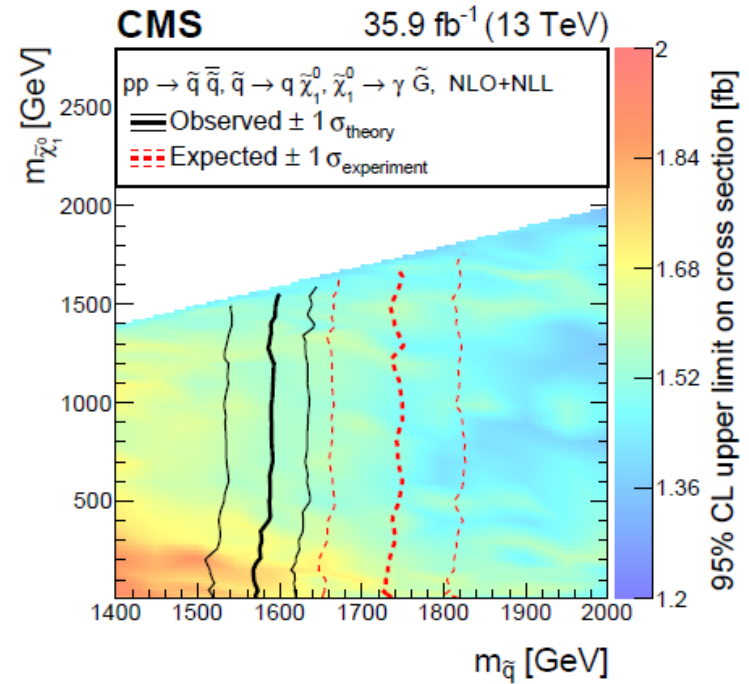
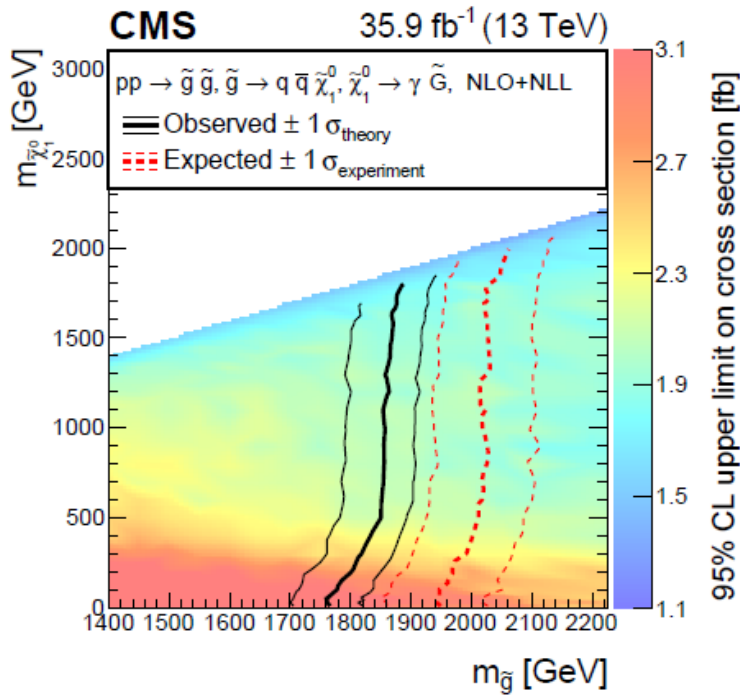
Estimated - Observed events for T5gg model at 35.9fb^{-1}



- Stack plot with QCD , EWK and $Z\gamma\gamma$ background estimates
- $\gamma\gamma E_T^{\text{miss}}$ distribution in signal region (E_T^{miss})
- in the final bin we observe an 1.91σ excess.
- rest of the bins are consistent with MC predictions

E_T^{miss} (GeV)	Exp QCD	Exp EWK	$Z\gamma\gamma$	Total	Observed
100 – 115	$99.0^{+12.4}_{-12.1}$	13.7 ± 4.2	1.3 ± 0.6	$113.9^{+13.1}_{-12.8}$	105
115 – 130	$32.8^{+7.0}_{-6.7}$	9.0 ± 2.7	1.1 ± 0.6	$42.9^{+7.5}_{-7.3}$	39
130 – 150	$18.8^{+5.1}_{-4.9}$	7.4 ± 2.3	1.1 ± 0.6	$27.3^{+5.6}_{-5.4}$	21
150 – 185	$9.9^{+3.6}_{-3.4}$	6.1 ± 1.9	1.3 ± 0.7	$17.4^{+4.1}_{-3.9}$	21
185 – 250	$3.1^{+1.9}_{-1.7}$	5.8 ± 1.8	1.3 ± 0.6	$10.2^{+2.7}_{-2.6}$	11
> 250	$1.0^{+1.1}_{-0.9}$	3.3 ± 1.1	1.1 ± 0.6	$5.4^{+1.6}_{-1.5}$	12

Mass Limits for gluino using 2.9fb^{-1}



Conclusions

- Full analysis is presented on 13TeV using 2016 data
- with 35.9 fb^{-1} we improved our sensitivity compared to 2015 analysis
- an excess of 1.9σ is observed in the final bin with respect to the standard model expectation
- exclude gluino masses below 1.86 TeV and squark masses below 1.59 TeV

This work is part of Garifallia Paspalaki's thesis in progress

Documentation

Search for general gauge mediated supersymmetry in events with photons, jets, and missing transverse momentum

A. Askew¹, A. Reinsvold Hall², M. Hildreth², A. Kyriakis³, T. McCauley², and G. Paspalaki¹

¹ Florida State University

² University of Notre Dame

³ National Center for Scientific Research Demokritos

Abstract

The results of a search for new physics in final states with photons and missing transverse momentum are reported. The study is based on a sample of proton-proton collisions collected at a center-of-mass energy $\sqrt{s} = 13$ TeV with the CMS detector in 2016. The integrated luminosity of the sample is 35.92 fb^{-1} . Many models of new physics, notably supersymmetry (SUSY) with general gauge mediation (GGM), predict the production of events with photons and significant missing transverse momentum. The data are used to search for GGM signatures in final states with two photons.

Search for supersymmetry in final states with photons and missing transverse energy in pp collisions at 13 TeV using the CMS detector

The CMS Collaboration

Abstract

Results are reported for a search for supersymmetry (SUSY) in final states with photons and missing transverse energy in proton-proton collisions at the CMS detector in 2016. The data sample corresponds to an integrated luminosity of 35.9 fb^{-1} collected at a center-of-mass energy of 13 TeV. The results are interpreted in the context of models of supersymmetry with general gauge mediation (GGM). Limits are set on gluino pair production and squark pair production in the GGM SUSY framework. Gluino masses below 1.86 TeV and squark masses below 1.59 TeV are excluded at a 95% confidence level.

CADI

- SUS-17-011
- AN-17-131

Historic Data Quality Monitor(HDQM)

Daniel Duggan¹, Francesco Fiori², Hassan Jalil³, Tomas Hreus⁴, Aristotelis Kyriakis⁵,
Dimitrios Loukas⁵, Alkis Papadopoulos⁵, Alessandro Rosi⁶, and Uridah Sami Ahmed³

¹ Fermi National Accelerator Laboratory (USA)

² National Taiwan University (TW)

³ National University of Sciences and Technology (PK)

⁴ Universitaet Zuerich (CH)

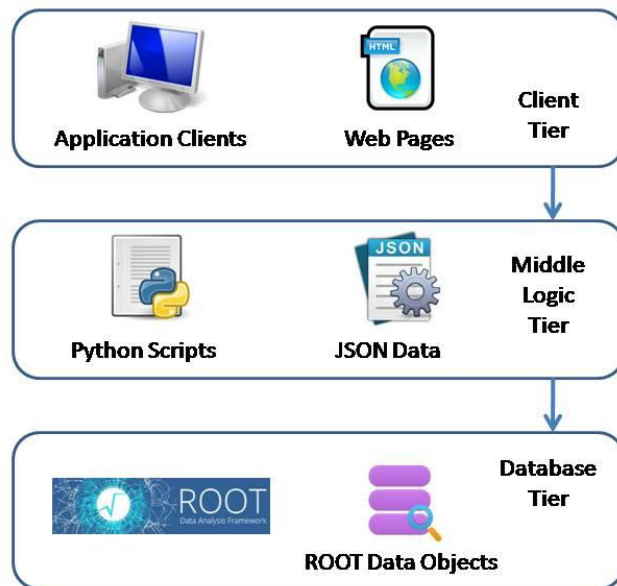
⁵ National Center for Scientific Research Demokritos (GR)

⁶ Universita e INFN, Perugia (IT)

Historic Data Quality Monitor(HDQM) (I)

➤The Historic Data Quality Monitor (HDQM) of the CMS experiment is a framework developed by the Tracker group of the CMS collaboration that permits a web-based monitoring of the time evolution of interesting quantities (i.e. signal to noise ratio, cluster size) in the Tracker Silicon micro-strip and pixel.

3 Tier Structure



GUI Web Interface in HTML + Javascript to display to extracted information

Python Scripts that extract the information from the Root files and save it to JSON type files

Data Base Tier: Root Events files

Python Scripts

- The python scripts that retrieve data from the official DQM and store them to JSON files:
 - `dconlyjson_all.py` → Checks the RR for Collision or Cosmic Good runs and provides a list of these runs
 - `Read_DCSONLY_JSON.py` → produces a map between the run number and the LHCFill number that the run belongs to.
 - `Get_Run_RunDuration_LHCFill_info.py` → produces a map between the run and its duration in seconds
 - `treadPlots_ROOTfile.py` → accesses the DQM root files and retrieves the trend data

JSON File Info

```
{
  "clusterStoN_ONTk_TIB_mpv": [
    {
      "run": 295315,
      "y": 18.1175,
      "x": 1.0,
      "hTitle": "S/N (mpv)",
      "yErr": 0.0032,
      "yTitle": "S/N (mpv)"
    },
    .....
  ]
}
```

WEB Interface

The screenshot displays the HDQM Web Interface. At the top, there are four dropdown menus for filters: '2017', 'StreamExpress', 'DECO', and 'Strips'. Below these, there is a 'Filter Runs' section with a 'Latest' dropdown, a '150' input field, and a 'Go to Correlation Plots' button. A row of checkboxes includes 'Show errors' (unchecked), 'Show fills' (checked), 'Show run duration' (checked), and 'Show regression lines' (checked). Below this is a 'Charts per page' dropdown set to '6' and a 'Submit' button. A red button labeled 'Short Help Instructions' is also present. The bottom section shows a grid of 20 variables, each with a checked checkbox. The variables are grouped into four columns: the first column (green background) contains clusterStoN variables; the second (orange) contains clusterStoN variables; the third (purple) contains T[OB/...] variables; and the fourth (blue) contains NAddressErr variables.

<input checked="" type="checkbox"/> clusterStoN_ONTk_TIB_L1_mpv	<input checked="" type="checkbox"/> clusterStoN_ONTk_TEC_PLUS_W1_mpv	<input checked="" type="checkbox"/> clusterStoN_ONTk_TID_MINUS_mpv	<input checked="" type="checkbox"/> T[OB/...]_GainsAAG_woG1G2_mpv
<input checked="" type="checkbox"/> clusterStoN_ONTk_TOB_L1_mpv	<input checked="" type="checkbox"/> clusterStoN_ONTk_TID_PLUS_R1_mpv	<input checked="" type="checkbox"/> clusterStoN_ONTk_TOB_mpv	<input checked="" type="checkbox"/> NAddressErr_APV_count
<input checked="" type="checkbox"/> clusterStoN_ONTk_TEC_MINUS_R1_mpv	<input checked="" type="checkbox"/> clusterStoN_ONTk_TID_MINUS_R1_mpv	<input checked="" type="checkbox"/> T[OB/...]_GainsAAG_mpv	<input checked="" type="checkbox"/> NAddressErr_APV_mean
<input checked="" type="checkbox"/> clusterStoN_ONTk_TEC_MINUS_W1_mpv	<input checked="" type="checkbox"/> clusterStoN_ONTk_TEC_MINUS_mpv	<input checked="" type="checkbox"/> T[OB/...]_GainsAAG_woG1_mpv	<input checked="" type="checkbox"/> Mean_NShot_Vs_Run
<input checked="" type="checkbox"/> clusterStoN_ONTk_TEC_PLUS_R1_mpv	<input checked="" type="checkbox"/> clusterStoN_ONTk_TIB_mpv	<input checked="" type="checkbox"/> T[OB/...]_GainsAAG_woG2_mpv	<input checked="" type="checkbox"/> Main_Diagonal_Position

Fig. 3. Main page of the HDQM Web Interface with a possible user selection related to the CMS Silicon Strip Tracker Detector.

Main developer: Alkis Papadopoulos

Trend Plots (Strip Tracker)

Silicon Strip Tracker related plot example

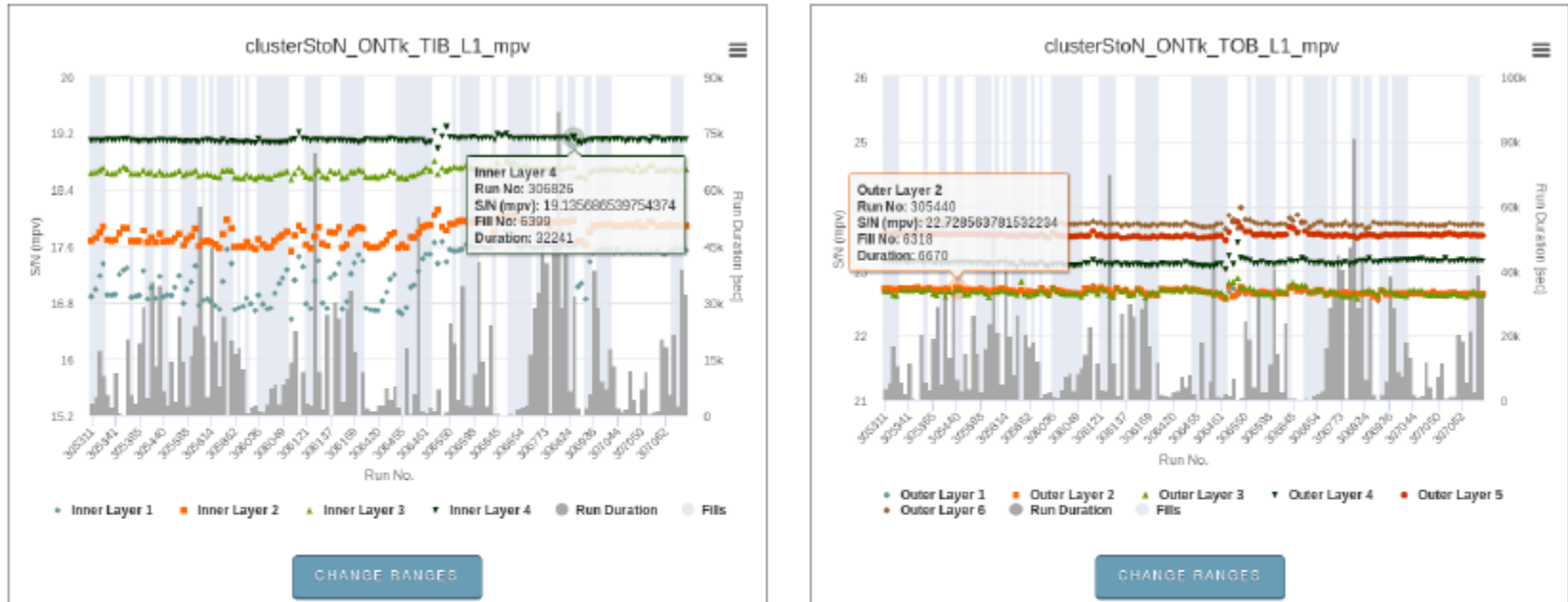


Figure 4: Example of two plots displaying the *Signal over Noise* of the *Tracker Inner Barrel* layers (left plot) and *Tracker Outer Barrel* layers (right plot). The white and grey zones of the runs that belong to the same LHC Fill number and the Run Duration in the right vertical axis are displayed. The pop up box with all the relevant information for a specific point of the graph is also shown.

Trend Plots (Pixel Tracker)

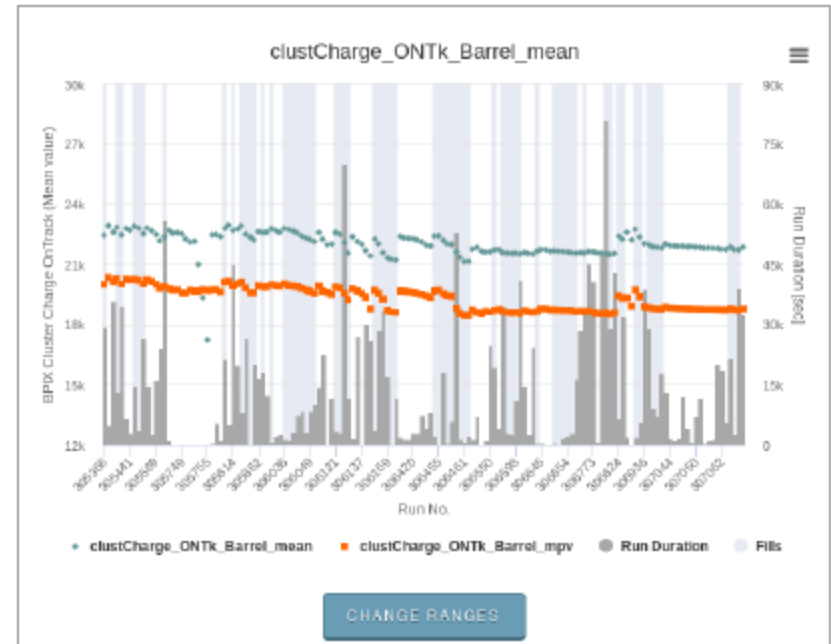
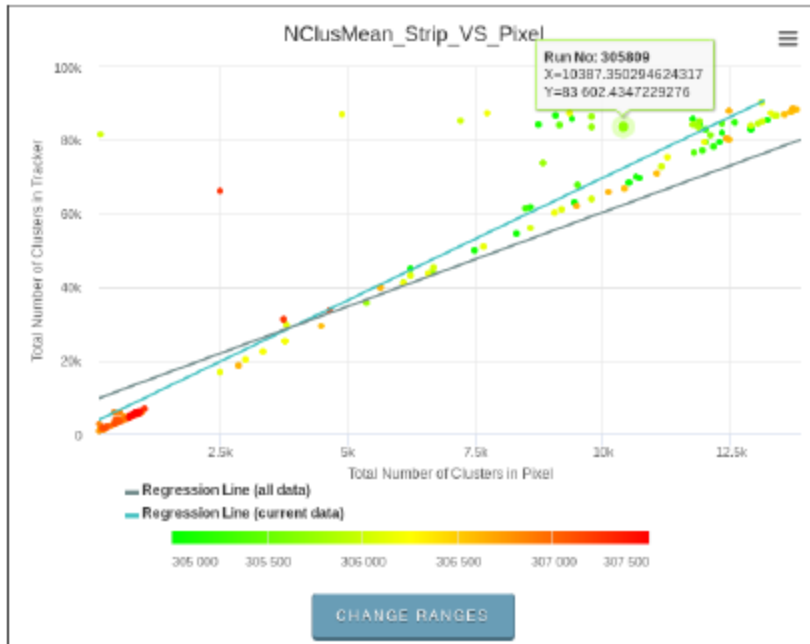


Figure 6: Example of two plots from *Pixel Phase1* detector displaying a 2D plot of the *Total Number of Clusters in Silicon Strip Tracker* versus the *Total Number of Clusters in Pixel* (left plot) and *Cluster Charge in Pixel Barrel* (right plot). The white and grey zones of the runs that belong to the same LHC Fill number and the Run Duration in the right vertical axis are displayed.

CMS Internal Note and CHEP2018 presentation

➤ The tool run smoothly during 2018 data taking period and was documented as an internal note and also presented in CHEP2018, Sofia Bulgaria

Available on CMS information server

CMS IN -2018/004

CMS Internal Note

The content of this note is intended for CMS internal use and distribution only

14 December 2017 (v5, 23 May 2018)

Historic Data Quality Monitor (HDQM) Tool for the CMS Tracker

Daniel Duggan^a, Francesco Fiori^b, Hassan Halil^c, Tomas Hreus^d, Aristotelis Kyriakis^e, Dimitrios Loukas^e, Alkis Papadopoulos^e, Alessandro Rossi^f, Uridah Sami Ahmed^g

^a Fermi National Accelerator Laboratory (USA), ^b National Taiwan University (TW), ^c National University of Sciences and Technology (PK), ^d Universitaet Zuerich (CH), ^e Nat. Cent. for Sci. Res. Demokritos (GR), ^f Universita e INFN, Perugia (IT)

Abstract

Monitoring the time evolution of sensitive quantities is fundamental to LHC experiments. It permits keeping control on data quality during LHC running and also effectively checking the influence on data of any detector calibration performed during the year. The Historic Data Quality Monitor (HDQM) of the CMS experiment is a framework developed by the Tracker group of the CMS collaboration that permits a web-based monitoring of the evolution of measurements (S/N ratio, cluster size) in the Tracker Silicon micro-strip and pixel detectors. The framework provides a way to build and deploy trend plots based on two steps of actions. In the first step data are retrieved from the offline DQM data base periodically via a cron scheduled job and a list of datasets is produced. In the second step, the web interface dynamically and interactively produces the trend plots from the datasets. The overall organization of the tool will be presented along with its internal structure and representative examples. Finally the skeleton for the flexible implementation of the HDQM in the other sub-detectors of the CMS experiments will be described.

To be published soon in the
[EPJ Web of Conferences](#)

Available on CMS information server

CMS CR -2018/285



The Compact Muon Solenoid Experiment Conference Report

Mailing address: CMS CERN, CH-1211 GENEVA 23, Switzerland



17 October 2018 (v3, 29 October 2018)

A Historic Data Quality Monitor (HDQM) tool for the CMS Tracker Detector

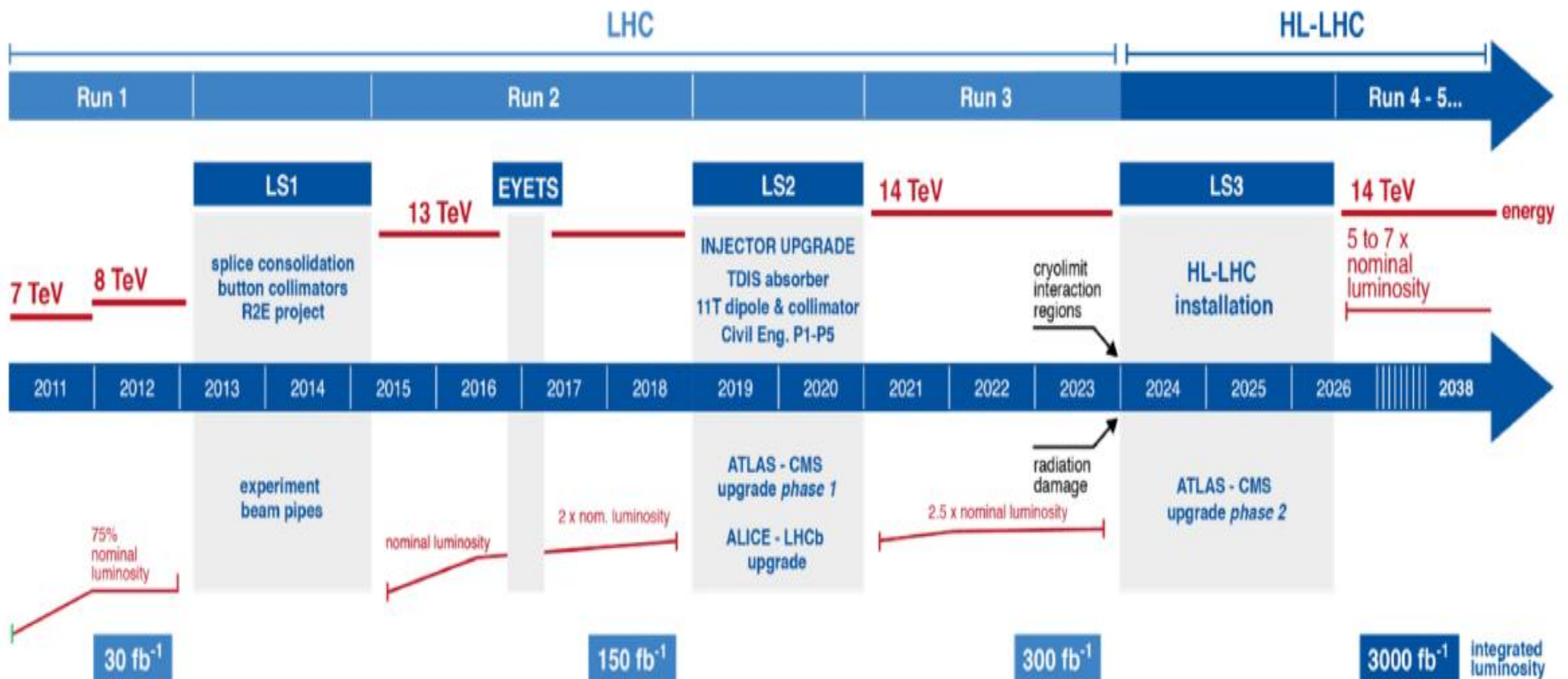
Aristotelis Kyriakis for the CMS Collaboration

Abstract

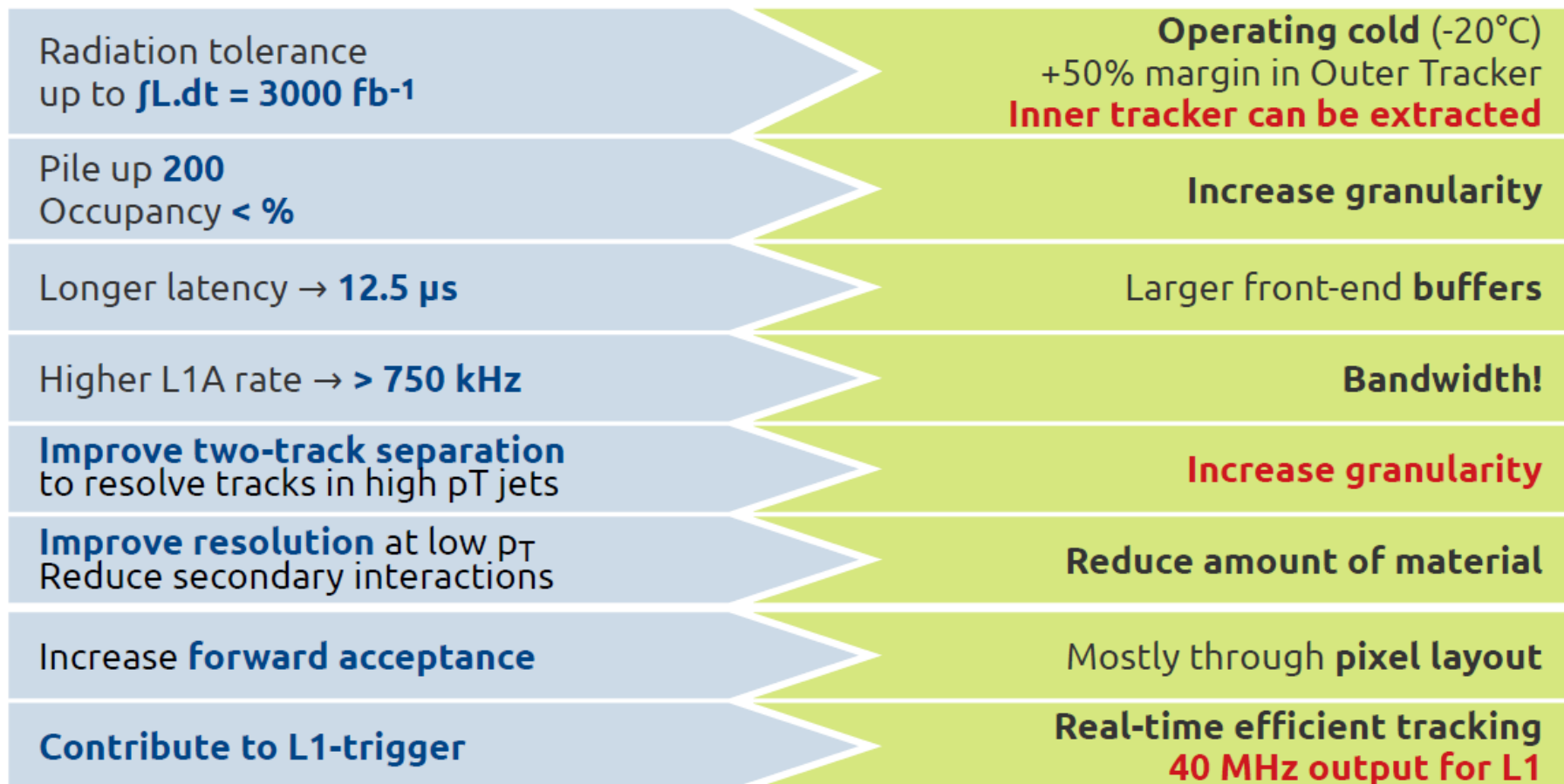
Monitoring the time evolution of data related observables is important for the successful operation of the LHC experiments. It permits keeping control on data quality during LHC running and also effectively checking the influence on data of any detector calibration performed during the year. The Historic Data Quality Monitor (HDQM) of the CMS experiment is a framework developed by the Tracker group of the CMS collaboration that permits a web-based monitoring of the time evolution of interesting quantities (i.e. signal to noise ratio, cluster size) in the Tracker Silicon micro-strip and pixel.

CMS Tracker Upgrade for HL-LHC

HL-LHC is on its way...



HL-LHC : CMS Tracker Total Tracker Replacement



HL-LHC : CMS Tracker Upgrade ...

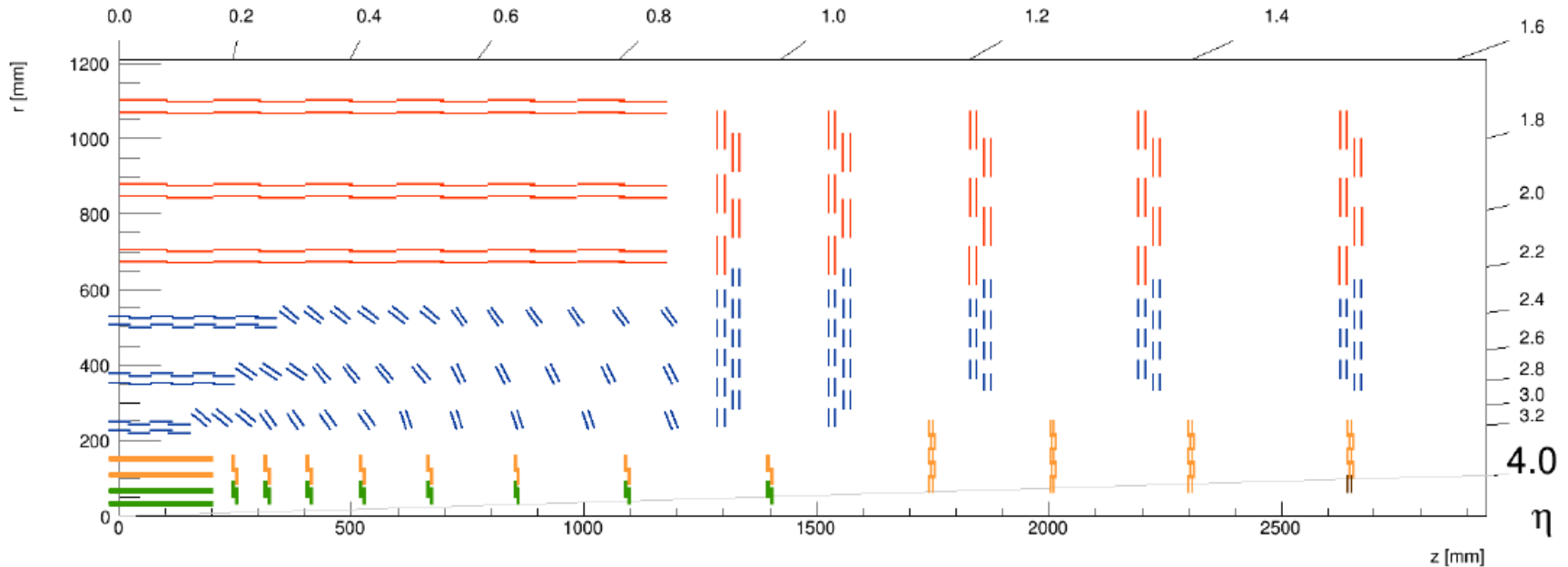
Current



HL-LHC

Outer Tracker	~200 m ²	Silicon surface	~190 m ²
	9.3 M	Strips	42.0 M
	–	MacroPixels	173 M
	15 148	Modules	13 296
	100 kHz	readout rate	750 kHz /40 MHz
Inner Tracker	~1 m ²	Silicon surface	4.9 m ²
	66 M	Pixels	2.0 G
	1440	Modules	4352
	100 kHz	readout rate	750 kHz

HL-LHC: CMS Tracker Layout



2 types of Outer Tracker:

- **2S (Strip-Strip sensor modules)**
- **PS (macro-Pixel Strip sensor modules)**

2 types of Inner Tracker modules

- **2×2 Pixel Chip modules**
- **2×1 Pixel Chip modules**

HL-LHC : CMS Tracker 2S Module

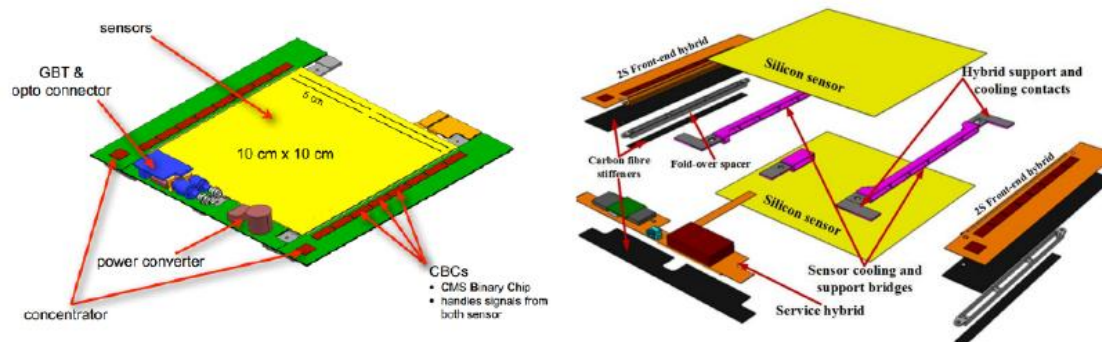
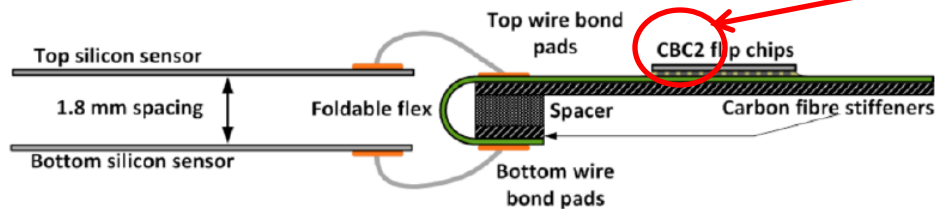


Figure 9.4: Strip - Strip (2S) module for the Outer Tracker in compact (left) and exploded view (right).



CMS Binary Chip(CBC) contains the STUB logic

Figure 9.5: Fold over and carbon fiber stiffeners of the Front - End hybrid in the Strip - Strip (2S) modules.

HL-LHC : CBC Test in Beam Tests

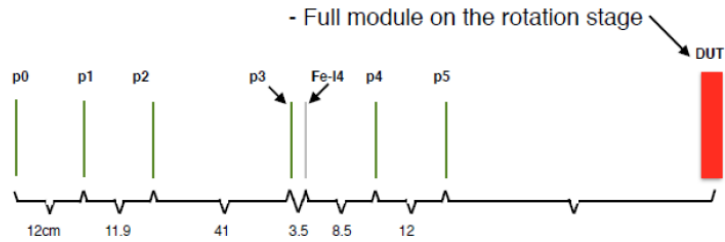


Figure 9.10: EU Telescope geometry and position of the Device Under Test (DUT) during November Beam-Test (BT).

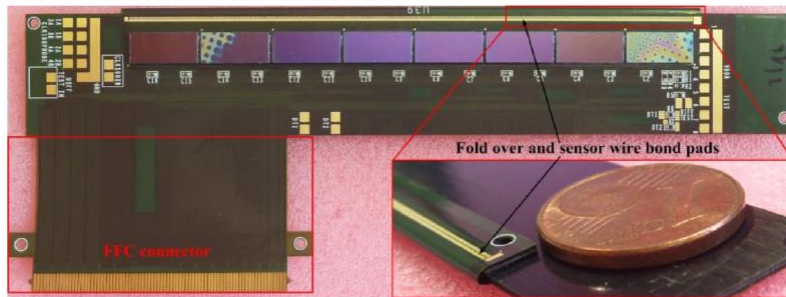
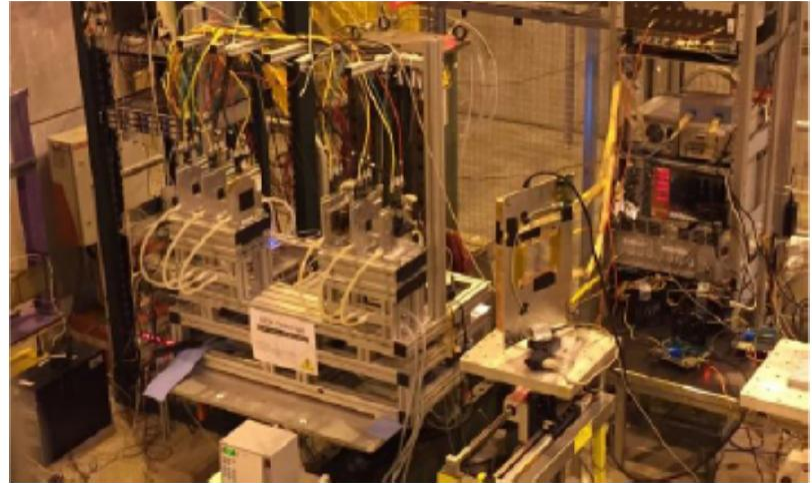
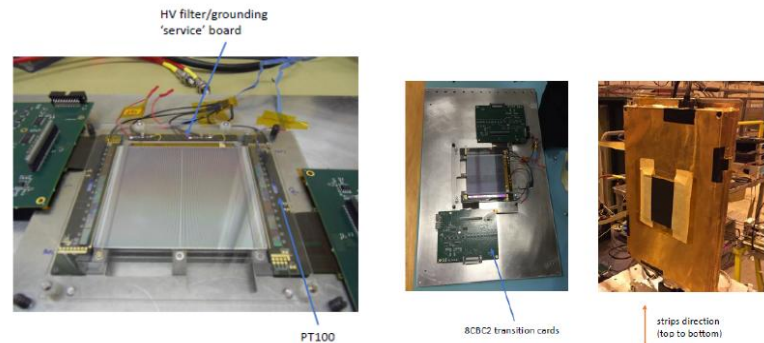


Figure 9.6: 8CBC2 flexible prototype and its folded wirebond pads.



HL-LHC : CBC Block Diagram & Calibration

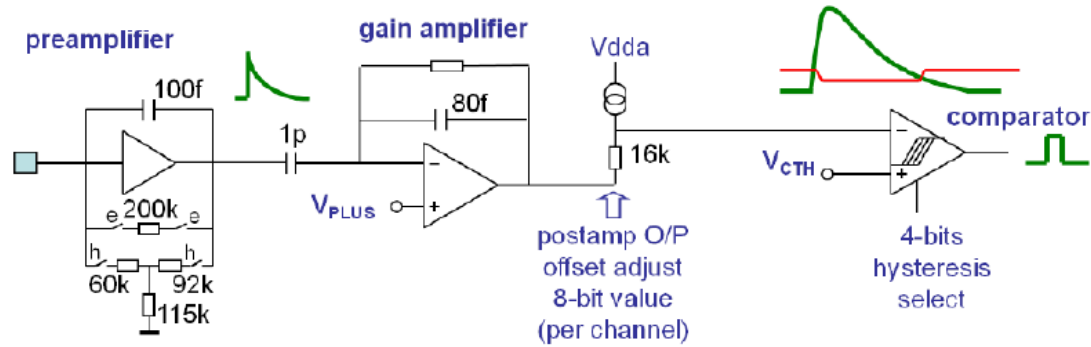


Figure 9.7: CBC2 analog path block diagram.

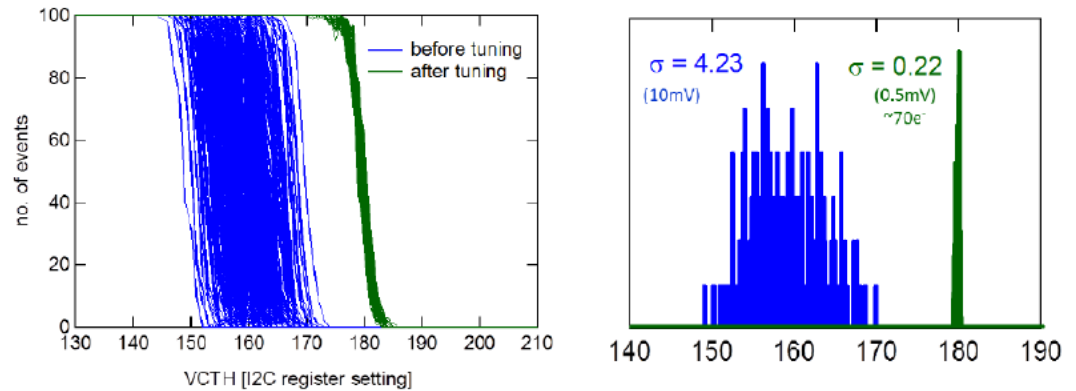


Figure 9.8: CBC2 S-curves calibration procedure plots.

HL-LHC : CBC STUB logic

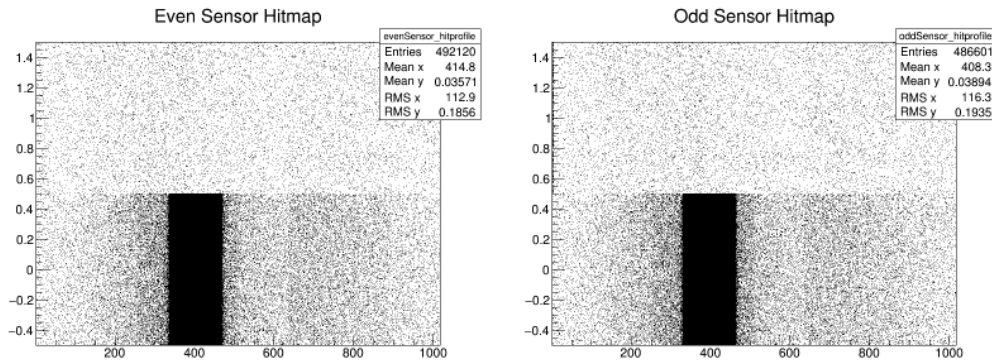
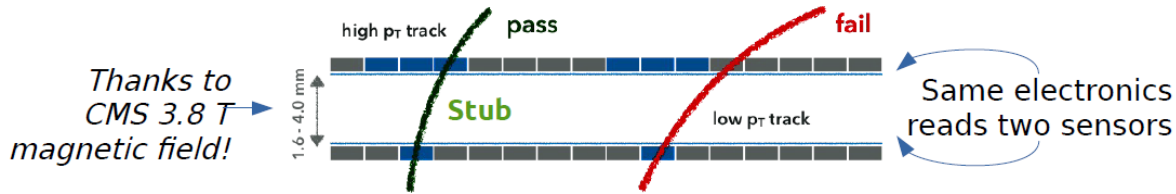
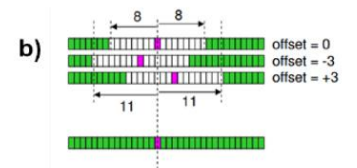
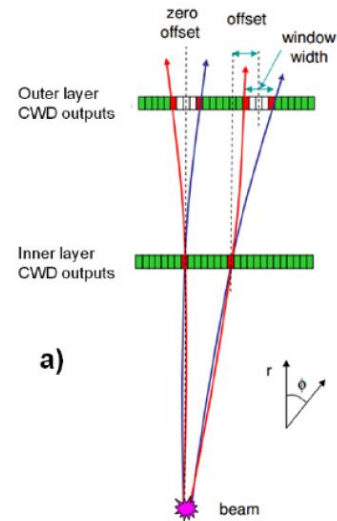


Figure 9.14: Raw hits on the sensors during November 2015 BT. Left, even sensors raw hits. Right, odd sensors raw hits. The upper half planes do not have many hits due to the beam not hitting in the center of the DUT.



HL-LHC : CBC STUB Production Rate vs rotation angle

One of the first results proving that the STUB logic of the CBC chip is working

$$\text{Rate} = \frac{\text{number of stubs}}{\text{number of events}}$$

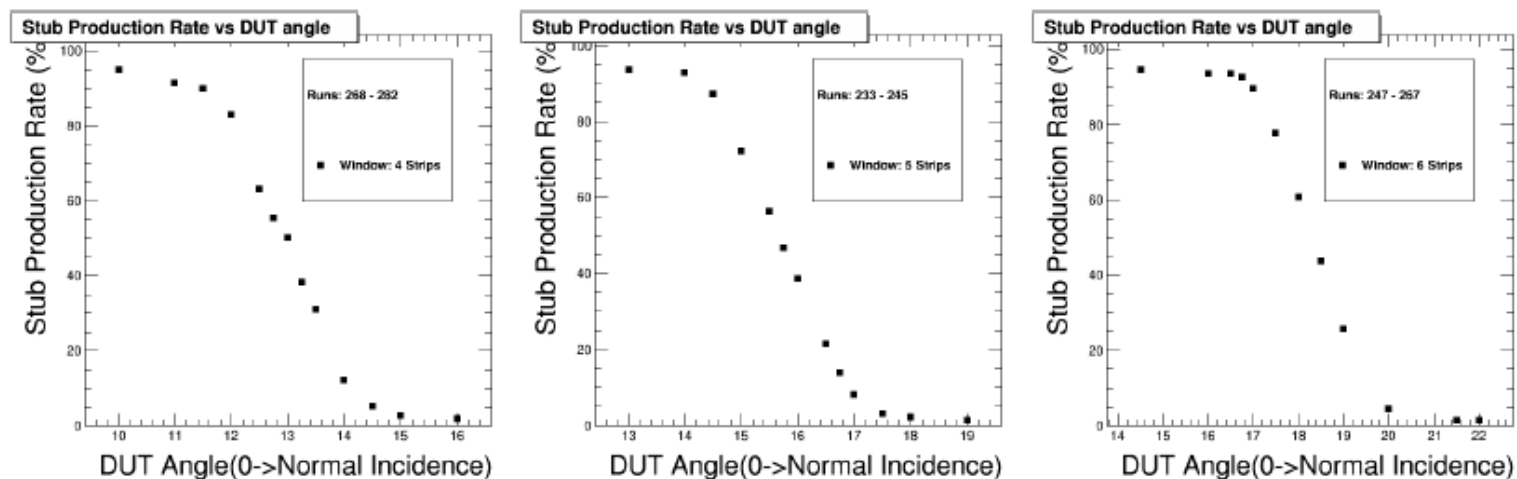


Figure 9.15: Stubs production rate versus the DUT angle, for four different allowance windows for the stub definition. Left, 4-strip window. Middle, 5-strip window. Right, 6-strip window.

HL-LHC : CBC STUB Production Rate at different CBSs

Check the STUB Production rate in different CBCs by moving the whole detector left – right of the beam direction

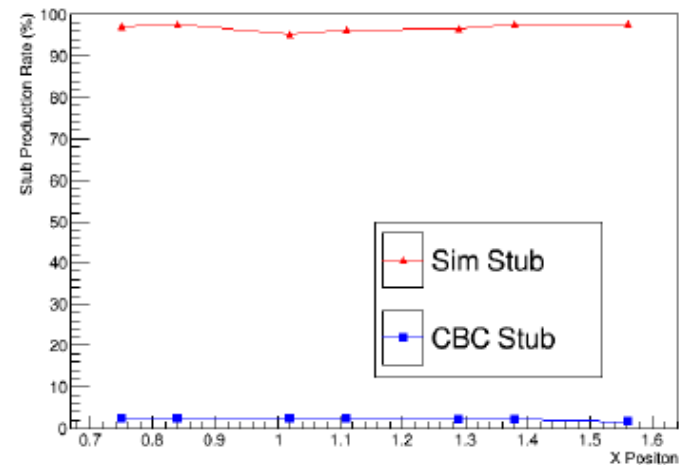
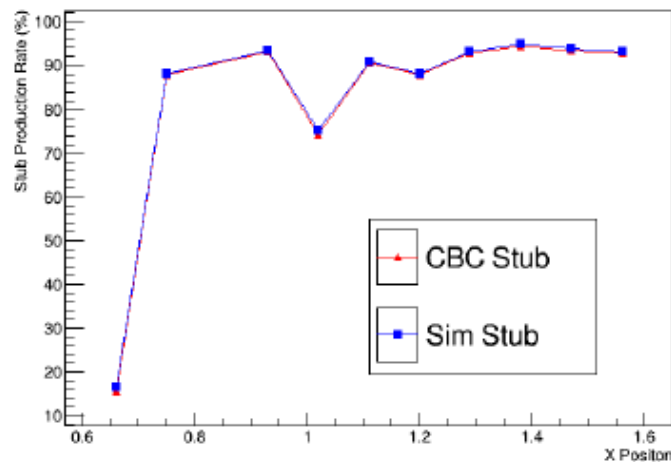


Figure 9.16: Stub production rate as a function of the x -position for the two sensor columns. Left for Column-0 and right for Column-1. Column-1 misbehaves possibly as a result of a FPGA readout board Firmware (GLIB) problem.

HL-LHC : CBC – Telescope Track matched efficiency

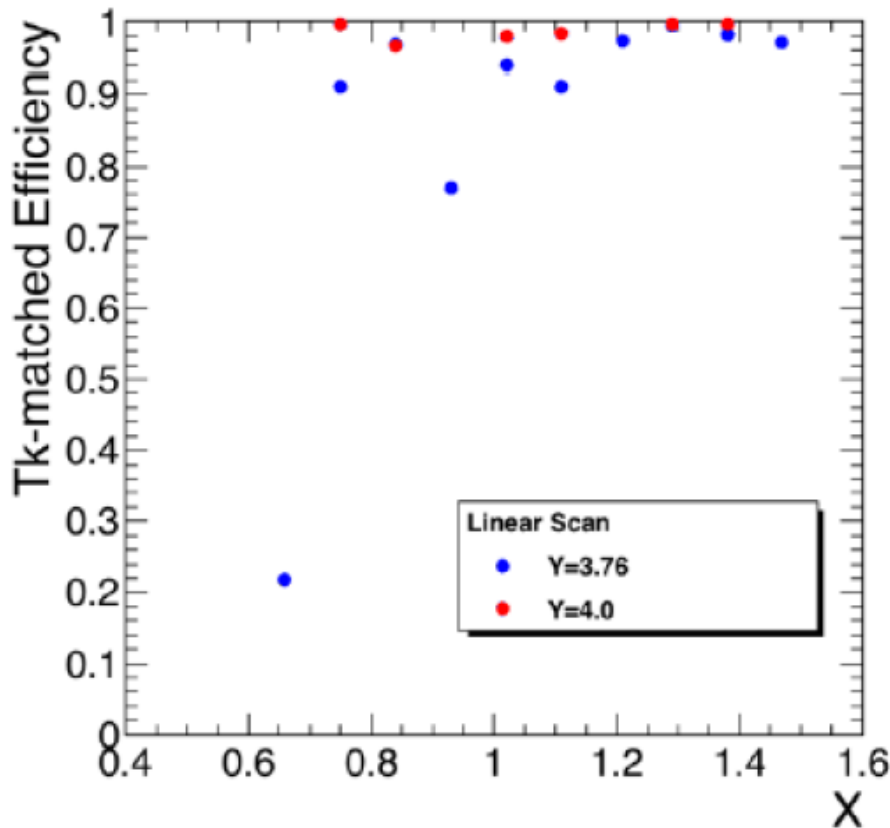


Figure 9.20: AIDA Telescope Track Efficiency.

HL-LHC : CBC Beam Test Note

2018/08/22

Head Id:

Archive Id: 471836:471839M

Archive Date: 2018/08/14

Archive Tag: trunk

Performance of Prototype Silicon Detectors for the Outer Tracker for the Phase II Upgrade of CMS

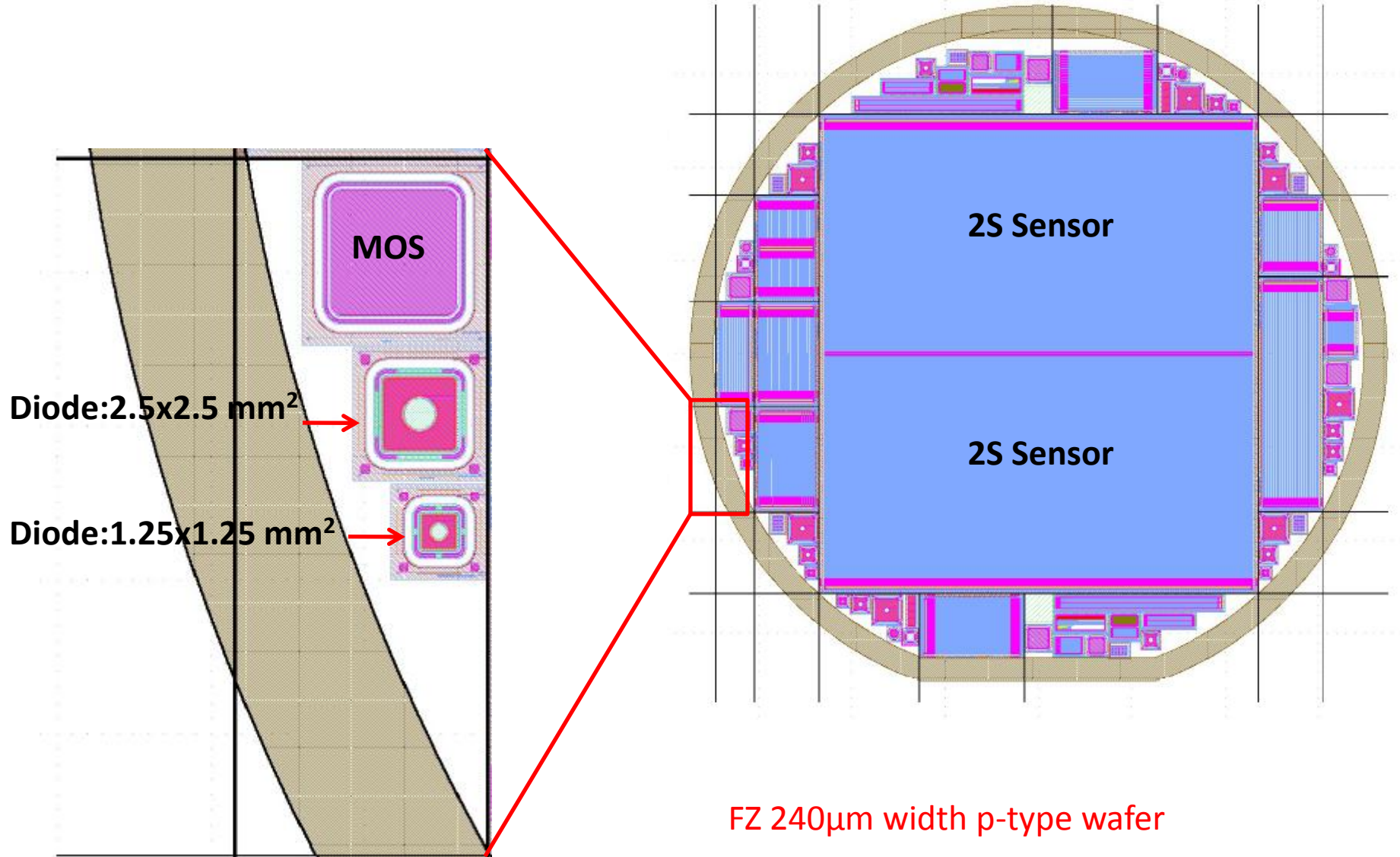
Jeremy Andrea¹, Georg Auzinger⁹, Rajarshi Bhattacharya³, Anadi Canepa⁴, Nicolas Pierre Chanon⁵, Vladimir Cherepanov¹, Nikkie Deelen², Martin Delcourt⁶, Alexander Dierlamm⁷, Suchandra Dutta³, Thomas Eichhorn¹¹, Tomasz Gadek², Yuri Gershtein¹⁰, Geoffrey Hall⁹, Mykyta Haranko¹¹, Siew Yan Hoh⁴, Alan Honma², Mark Kovacs², Stefano Mersi², Alan Prosser⁴, Nabin Poudyal¹², Robert Harr¹², Ryan Rivera⁴, Alessandro Rossi¹³, Suvankar Roy Chowdhury³, Subir Sarkar³, Sarah Seif El Nasr¹⁴, Basil Schneider⁴, Jarne Théo De Clercq¹⁵, Jelena Luetic¹⁵, Lorenzo Uplegger⁴, Giovanni Zevi Della Porta¹⁶, Panagiotis Assiouras¹⁷, Aristoteles Kyriakis¹⁷, and Dimitrios Loukas¹⁷

¹ Universit de Strasbourg² CERN³ Saha Inst. of Nucl. Phys., Kolkata⁴ Fermilab⁵ Univ. de Lyon⁶ Univ. Catholique de Louvain⁷ Inst. fr Exp. Teilchenphysik, Karlsruhe⁸ RWTH Aachen Univ.⁹ Imperial College, London¹⁰ Rutgers University¹¹ DESY¹² Wayne State University¹³ INFN Sez.; Univ. di Perugia¹⁴ Univ. of Bristol¹⁵ Vrije Univ. Brussel¹⁶ University of California San Diego¹⁷ Institute of Nuclear and Particle Physics, NCSR DEMOKRITOS

Abstract

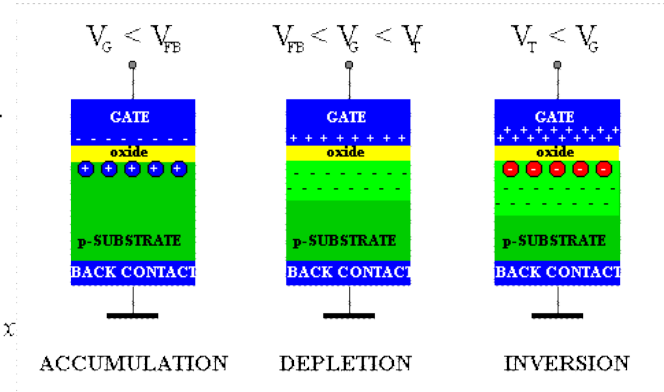
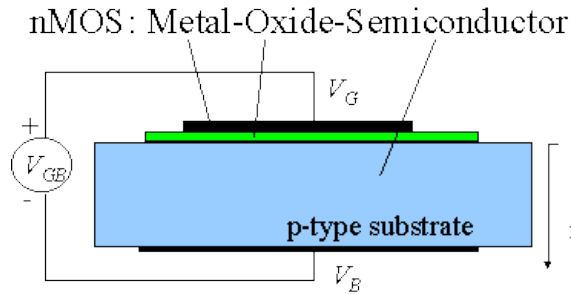
A new CMS Tracker is will be installed for the operation at the High Luminosity phase of LHC (HL-LHC). The detector modules and the readout electronics are specially designed to select high $p_T (> 2 \text{ GeV})$ track candidates and reduce the data volume before data transmission to the first level trigger. The inclusion of tracking information in the trigger decision is essential to select events of interest efficiently. A customized front-end readout chip (CBC), has been designed for this purpose, containing logic to correlate hits in pairs of microstrip sensors. The performance of such prototype modules put to test using beam is presented.

HL-LHC : 8" wafer with 2S Sensors

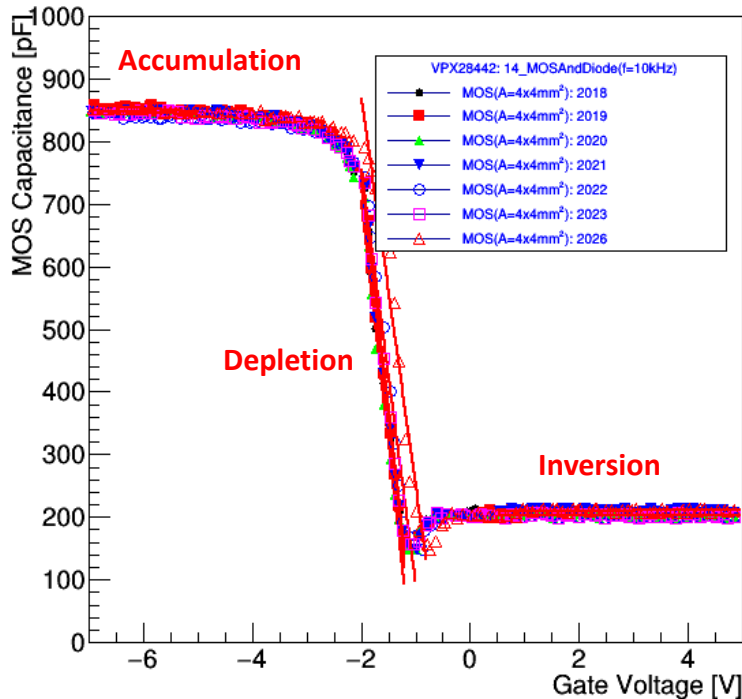


HL-LHC : CV MOS measurements

MOS standard, CV (AC pulse: 10 kHz, 0.25V), VPX28441, chip 14, $A = 4 \times 4 \text{ mm}^2$



Capacitance vs Voltage



MOS Id	C_{acc} [pF]	C_{inv} [pF]	d_{ox} [μm]	$-V_{FB}$ [V]	N_A [10^{12} cm^{-3}]
2018	847.1	210.7	0.652	1.64	6.04
2019	821.3	210.7	0.672	1.61	5.89
2020	847.1	202.5	0.652	1.69	6.51
2021	847.1	210.7	0.652	1.63	6.04
2022	809.7	202.5	0.682	1.52	5.91
2023	826.7	202.5	0.668	1.59	5.85
2026	818.2	208.2	0.675	1.37	7.18

Non radiated MOS CV curve

Our Measurements Compatible with other LAB

HL-LHC : CV MOS measurements – Other Parameters

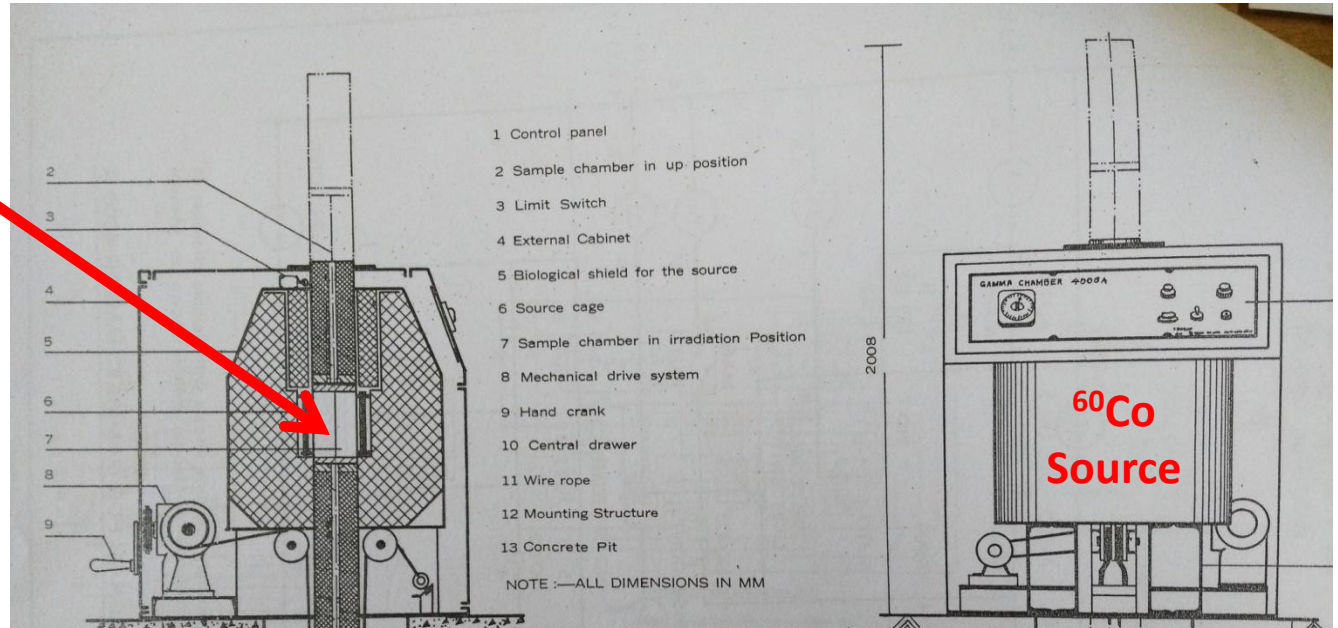
Example of other interesting quantities that can be extracted:

- Extrinsic Debye Length (λ_D) = 0.000161914 [cm] = 1.61 [μm]
- C_{Debye} = 1021.94 [pF]
- Flatband Capacitance (C_{FB}) = 462.662 [pF]
- Bulk Potential (ϕ_B) = -0.154246 [V]
- Metal - Semiconductor Work Function (W_{MS}) = -0.764246 [V]
- Threshold Voltage (V_{TH}) = -1.06483 [V]

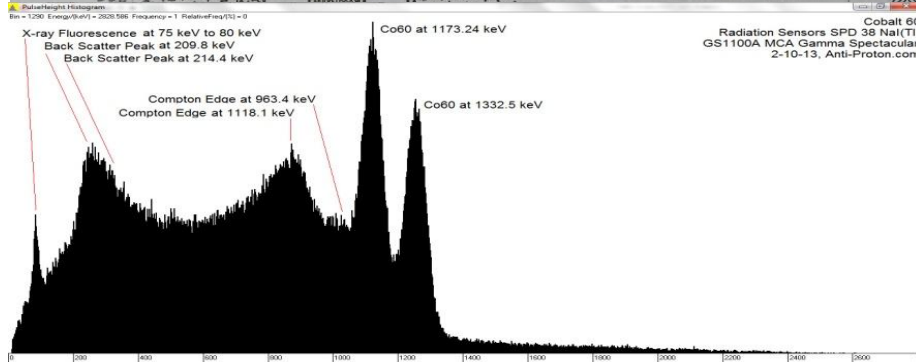
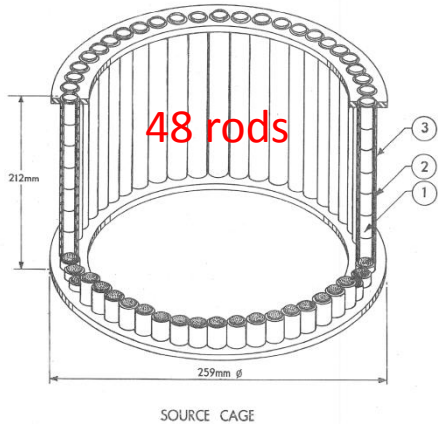
HL-LHC : Irradiation Procedure

Total Dose Expected at R = 60cm around 100KGy after 10 years at HL-LHC

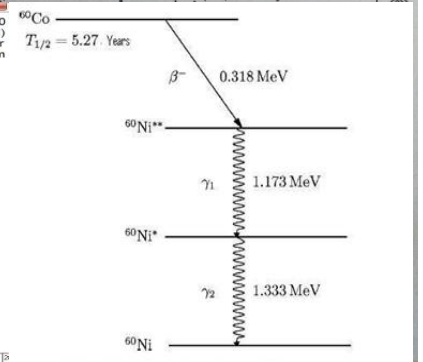
Irradiation Chamber



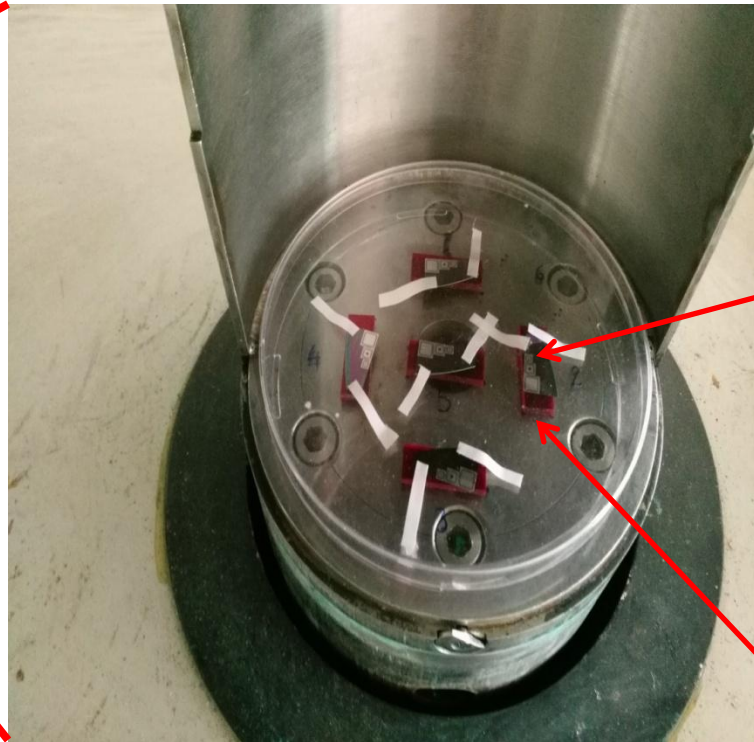
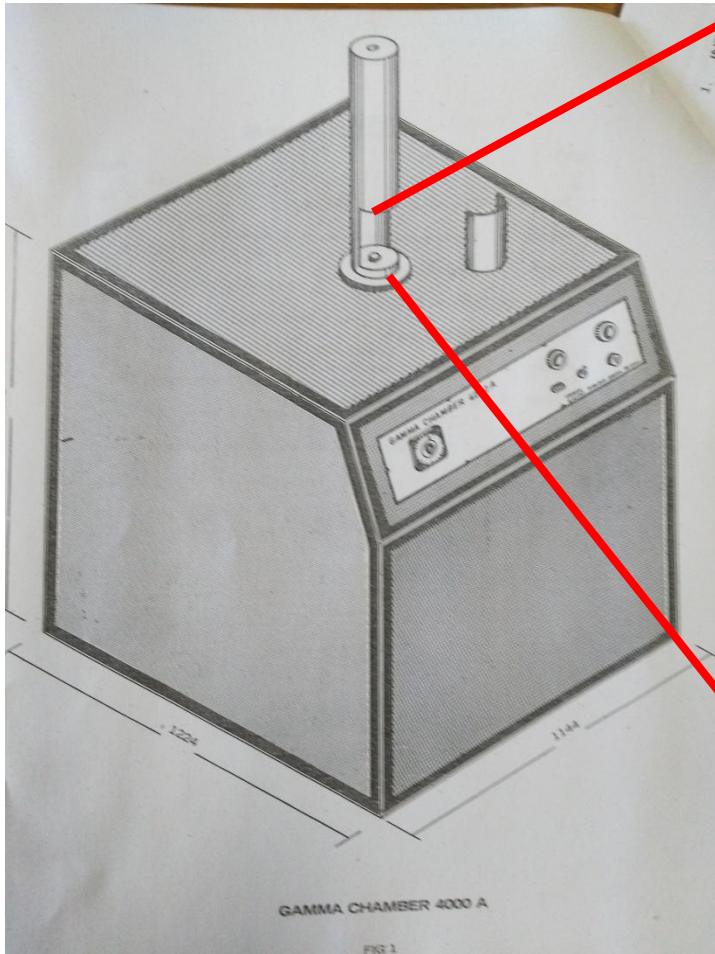
- ① Source
- ② Source pencil
- ③ Source pencil holder



Radiation Sensors SPD 38 NaI(Tl)
 GS1100A MCA Gamma Spectacular
 2-10-13, Anti-Proton.com



HL-LHC : Irradiation facility

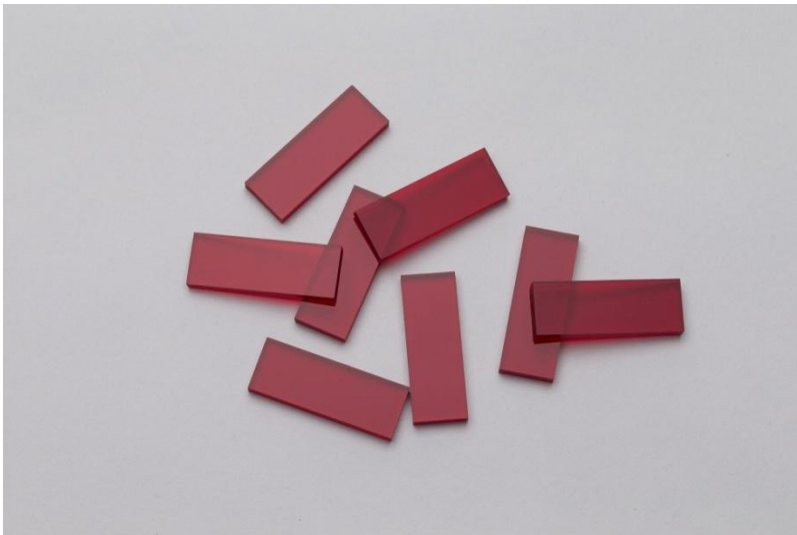


14-MOS
& Diodes,
Half
Diodes
and
Quarter
Diodes

Dosimeters -
PMMA

HL-LHC : PMMA Dosimeters

<http://www.harwell-dosimeters.co.uk/harwell-red-4034/>

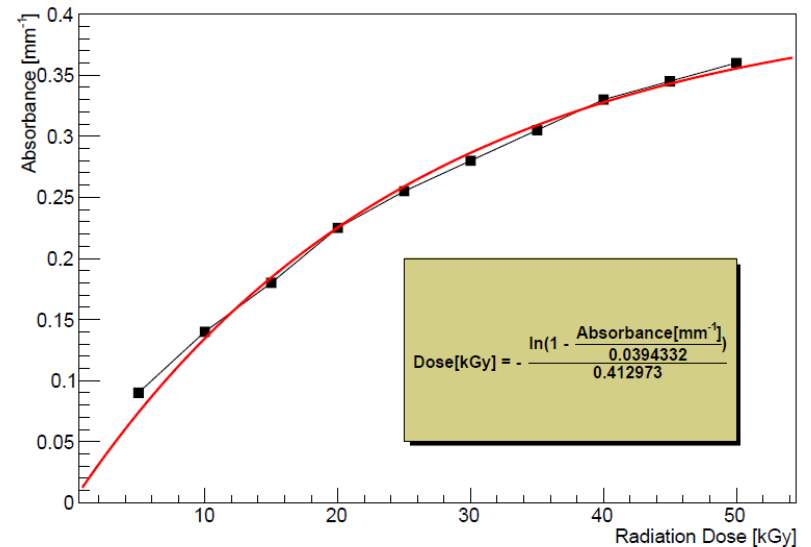


PMMA dimensions:
30mm x 10mm x 3mm

Maximum Accepted Dose : 5 - 50kGy

- 1) Use Optospectrometer to measure the absorbance of PMMAs at $\lambda = 640\text{nm}$
- 2) Use the curve below to estimate the Radiation Dose

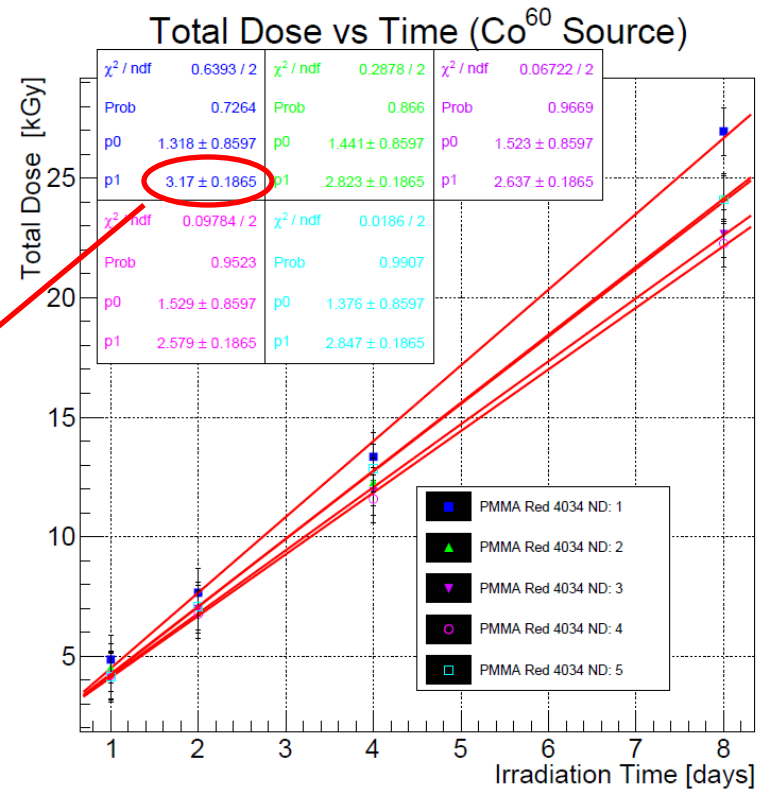
Harwell PMMA Red 4034 ND Perspex Dosimeter



HL-LHC : Dose Measurement

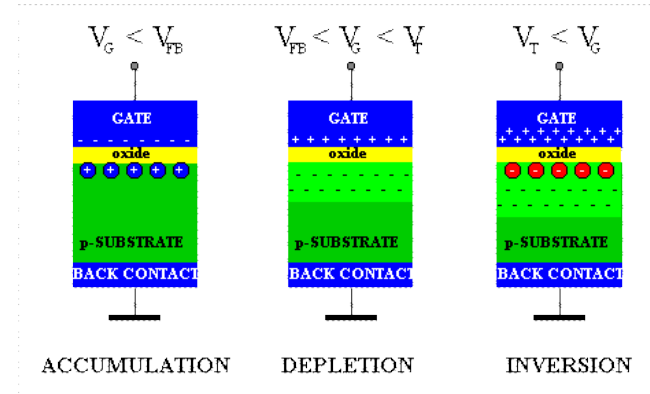
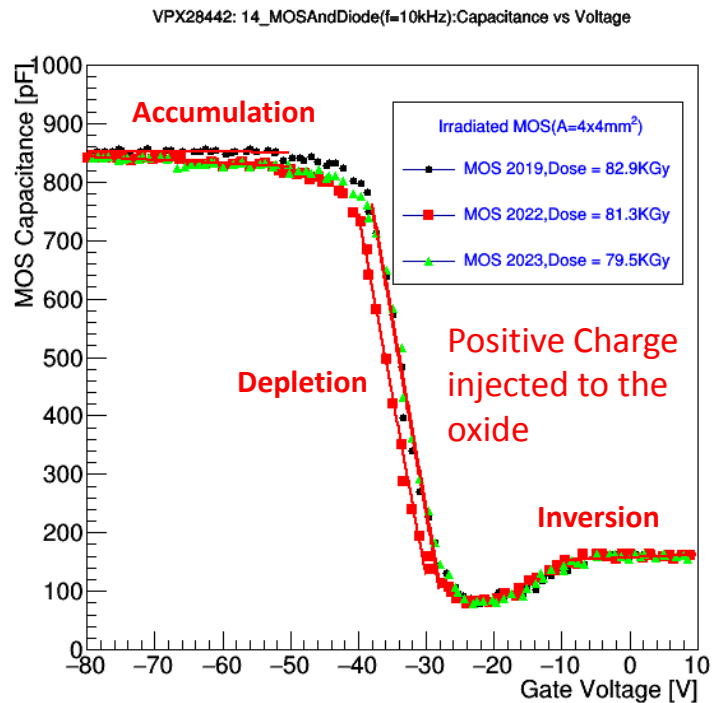
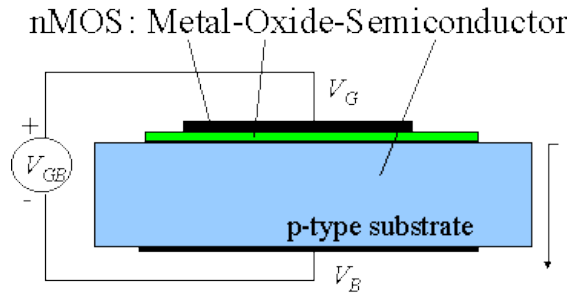


Position 1: MOS&Diode ID 2020 -> 3.17kGy/day
 Position 1: MOS&Diode ID 2021 -> 2.82kGy/day
 Position 1: MOS&Diode ID 2022 -> 2.67kGy/day
 Position 1: MOS&Diode ID 2023 -> 2.58kGy/day
 Position 1: MOS&Diode ID 2019 -> 2.85kGy/day



HL-LHC : CV MOS measurements (After Irradiation in ^{60}Co)

MOS standard, CV (AC pulse: 10 kHz, 0.25V),
 VPX28441, chip 14, $A = 4 \times 4 \text{ mm}^2$



MOS Id	Dose [KGy]	C_{acc} [pF]	C_{inv} [pF]	d_{ox} [μm]	$-V_{FB}$ [V]	N_A [10^{13} cm^{-3}]
2019	82.9	846.6	157.5	0.652	35.6	2.65
2022	81.3	789.2	158.1	0.700	37.2	2.69
2023	79.5	798.8	175.5	0.691	35.1	2.56

Irradiated MOS CV curve

HL-LHC : IV Diode measurements – Irradiation

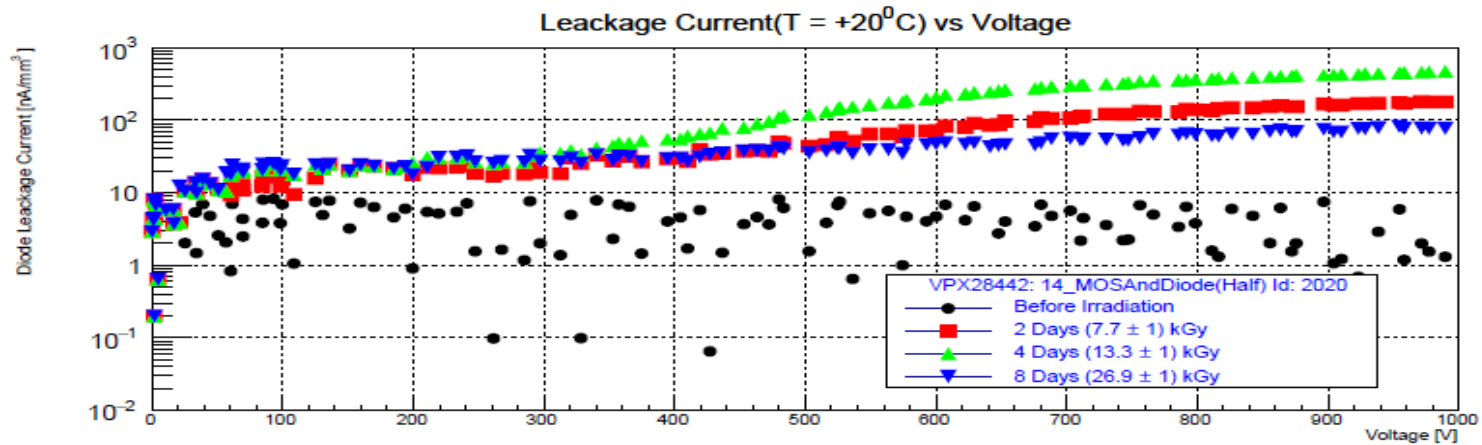
- Since we had to share the Irradiation Facility we were not able to follow a specific annealing protocol

Irradiation time[days]	Accumulated Irradiation time [days]	Annealing Time at room temperature [days]
2	2	13
2	4	2
4	8	2

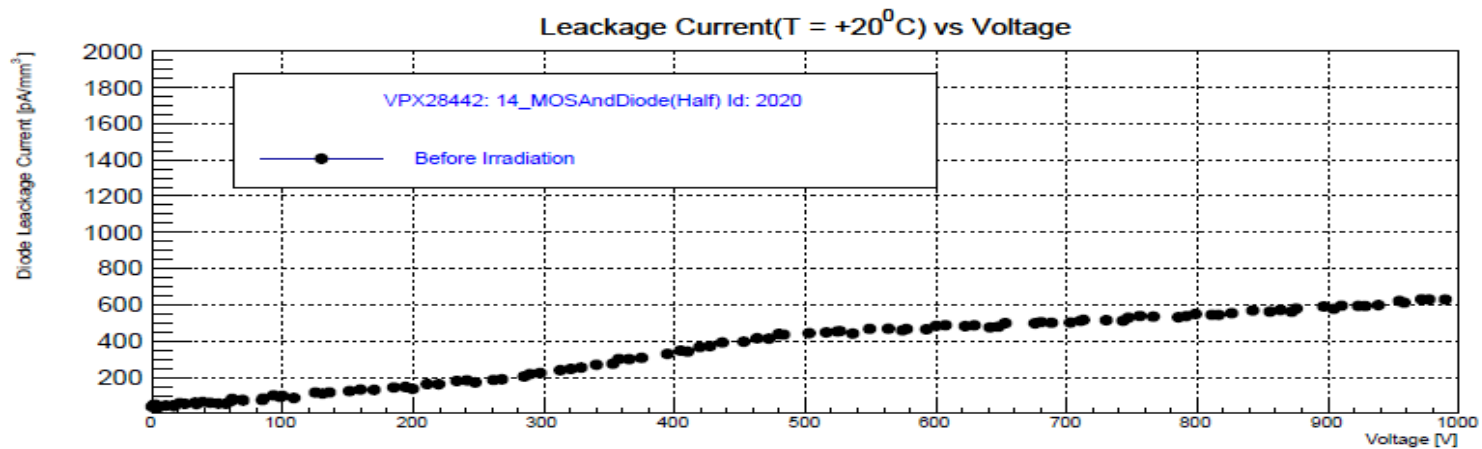
➤ $I(20^{\circ}\text{C}) = I(T) * (293/T)^2 * \exp[-1.21/k_B * (1/293 - 1/T)]$, **RD50 TN 2011-01**

HL-LHC : IV measurements Irradiated Half Diode

2020

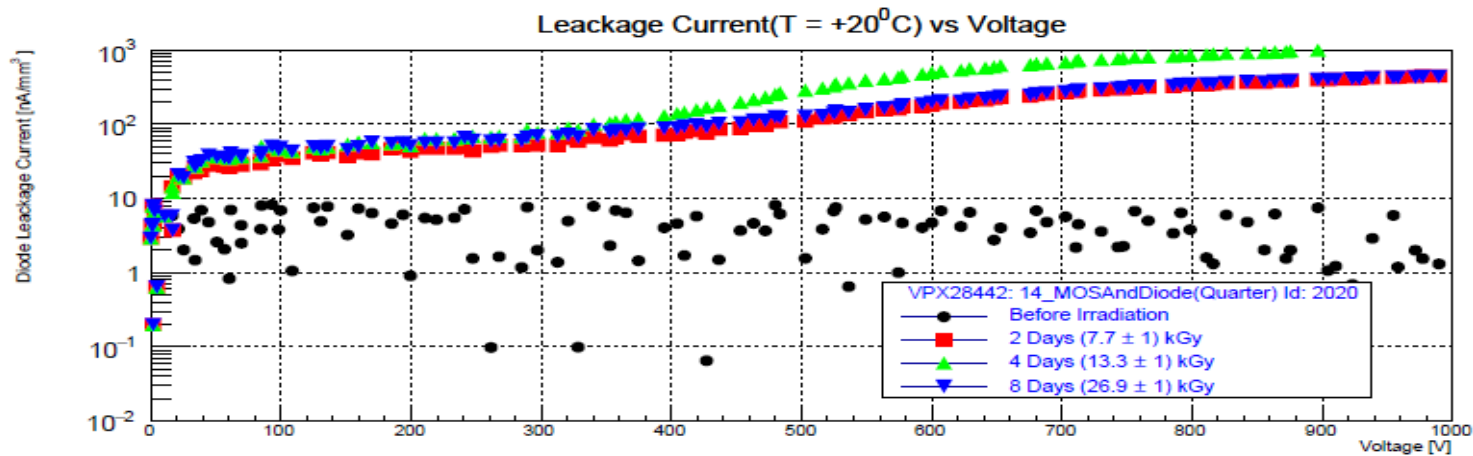


Half Diodes
dimensions:
2.5mm x
2.5mm x
0.24 mm

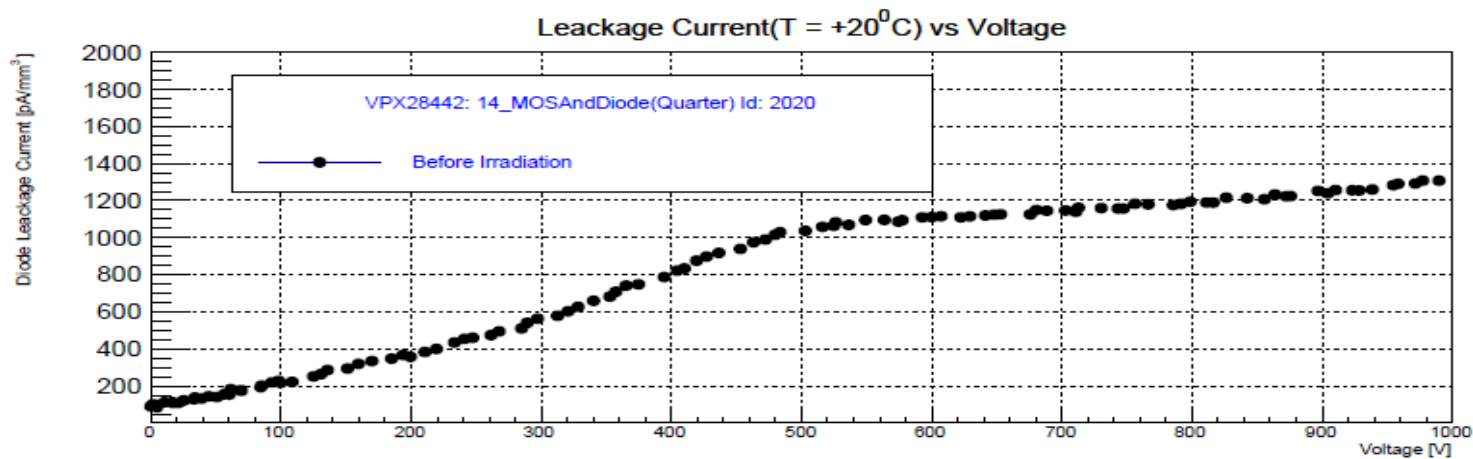


HL-LHC : IV measurements Irradiated Quarter Diode

2020



Quarter
Diodes
dimensions:
1.25mm x
1.25mm x 0.24
mm



Radioactive Source Localization

G. Fragos¹, C. Karafasoulis², A. Kyriakis³, C. Potiriadis⁴, I. Topsis-Giotis³

¹Hellenic Army General Staff R&IT Directorate

²Hellenic Army Academy

³*Institute of Nuclear and Particle Physics, NCSR “Demokritos”*

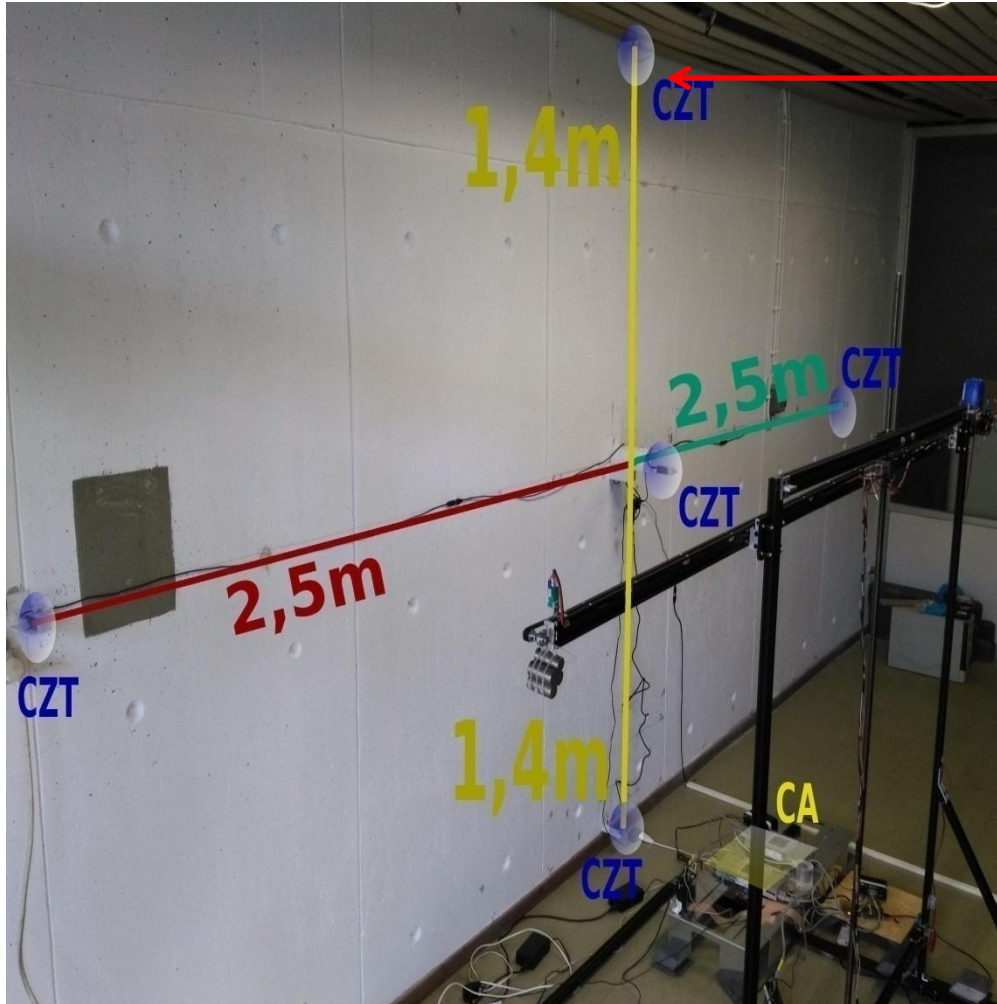
⁴*Greek Atomic Energy Commission*

Funded by NATO, Sfp-984705, 400KEuros

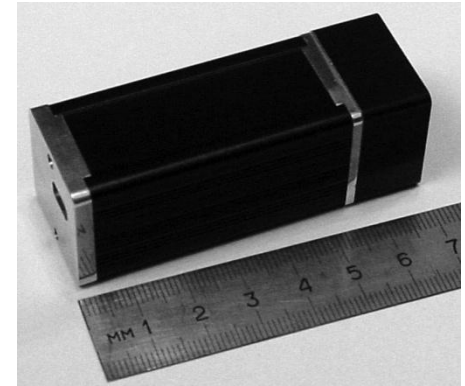
Introduction - Main Idea

- Radiation Source Localization is a very hot research topic and the project aims to develop core technologies of distributed sensor networks for the localization and isotope identification of radioactive sources with purpose to build a solution applicable to the diverse problems which one confronts when dealing with difficult to detect (either shielded or in a large crowd) sources in spaces without specific entrance and exit points.

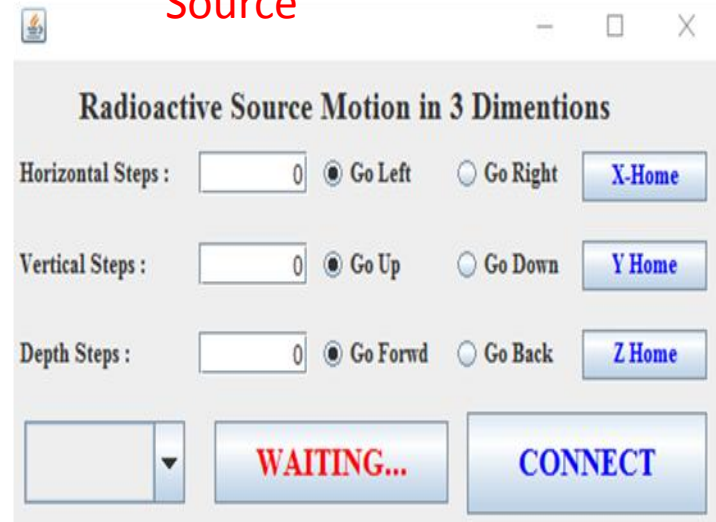
Test Bed Setup



CZT
Sensors

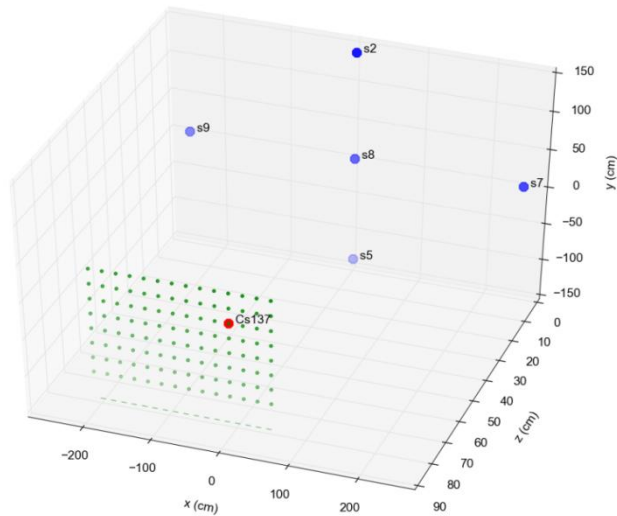


^{137}Cs
Radioactive
Source

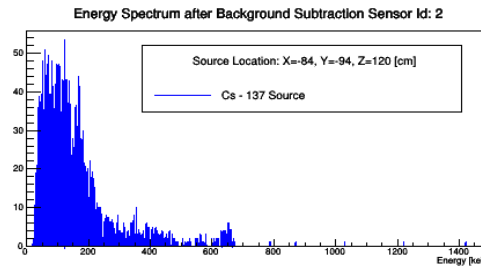


Motion Control GUI

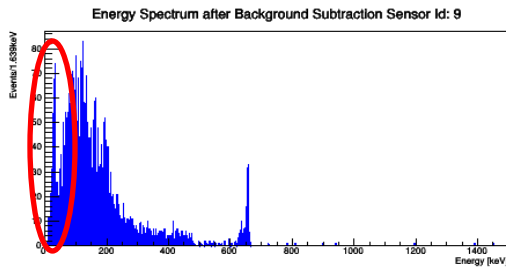
System Response for an unshielded ^{137}Cs Source



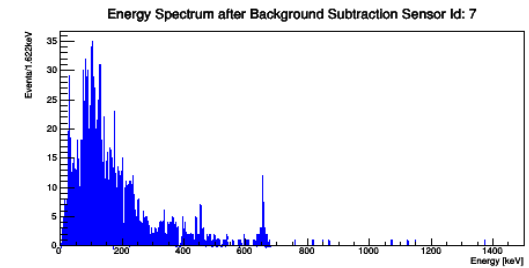
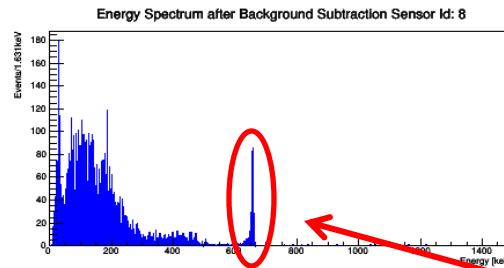
^{137}Cs Source



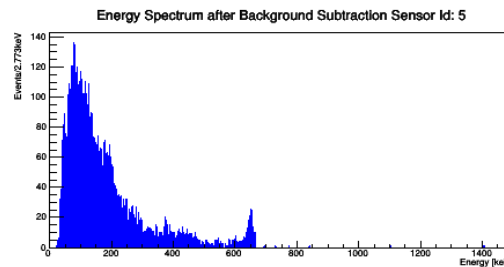
Source Activity :
6.7MBq~180 μCi



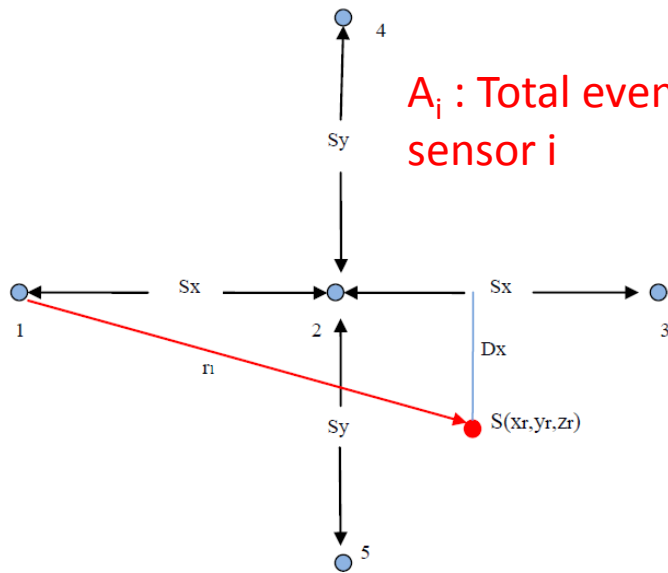
X-ray : 32keV



γ -ray : 662keV



Localization Based on Analytical Calculations



A_i : Total events recorded by sensor i

$$q_1^x = \frac{r_1^2}{r_2^2} = \frac{A_2}{A_1} = \frac{(x_r + S_x)^2 + D_x^2}{x_r^2 + D_x^2}$$

$$q_2^x = \frac{r_3^2}{r_2^2} = \frac{A_2}{A_3} = \frac{(S_x - x_r)^2 + D_x^2}{x_r^2 + D_x^2}$$

$$x_r = \frac{S_x(q_1^x - q_2^x)}{2(q_1^x + q_2^x) - 4}$$

$$q_1^y = \frac{r_5^2}{r_2^2} = \frac{A_2}{A_5} = \frac{(y_r + S_y)^2 + D_y^2}{y_r^2 + D_y^2}$$

$$q_2^y = \frac{r_4^2}{r_2^2} = \frac{A_2}{A_4} = \frac{(S_y - y_r)^2 + D_y^2}{y_r^2 + D_y^2}$$

MVA : NN and BDT also used, Results are similar

$$z_r^1 = \sqrt{D_x^2 - y_r^2}$$

$$y_r = \frac{S_y(q_1^y - q_2^y)}{2(q_1^y + q_2^y) - 4}$$

DAQ Server GUI



Data Acquisition (DAQ) and Analysis Framework

Sensors Measurement Sessions Session Details Tools Step Motors

Registered sensors					
Id	Type	IP	Port	Latest response	
2	RITEC	10.0.1.234	6002	100 REPETITION 3 OF 9	
5	RITEC	10.0.1.234	6005	100 REPETITION 3 OF 9	
7	RITEC	10.0.1.234	6007	100 REPETITION 3 OF 9	
8	RITEC	10.0.1.234	6008	100 REPETITION 3 OF 9	
9	RITEC	10.0.1.234	6009	100 REPETITION 3 OF 9	

Refresh Clear Sensors

Commands

PING TIME

Source:	Cs-137	Source Longitude:	-104.5	Sensor X:	250
Repetitions:	9	Source Latitude:	-54.0	Sensor Y:	140
Acquisition time:	20 secs	Source Altitude:	120.0	Sensor Z:	0

Comments:
TANDEM Cs-137, RITEC(2,5,7,8,9), X=-104.5cm, Y=-54cm, Z=120cm. RUN= spectra 20s, 9 Repetitions SB_intercalibration = 1.3, On The Fly Localization - Record with CamStudio

LOOP

Sensor inter-calibration

Energy threshold
Between 20 keV and 3000 keV

Localization Algorithm
Select background measurement
857 : RITEC(Positions 2,5,7,8,9) Cross Topology - Background(20sec:x9rep)- 22/11/2018 - Sensor On The Fly Localization - Server 4.2 - Start

40 secs	X	Y	Z
Actual	-104.5	-54.0	120.0
Estimated	-97.98	-40.28	119.69
Diff	6.52	13.72	0.31

Localization Algorithm log

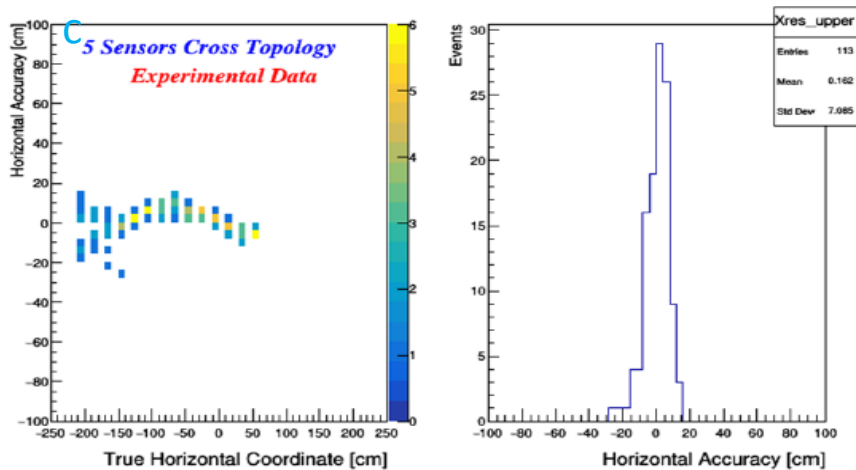
Horizontal and Vertical Sensor Distance

Source Localization

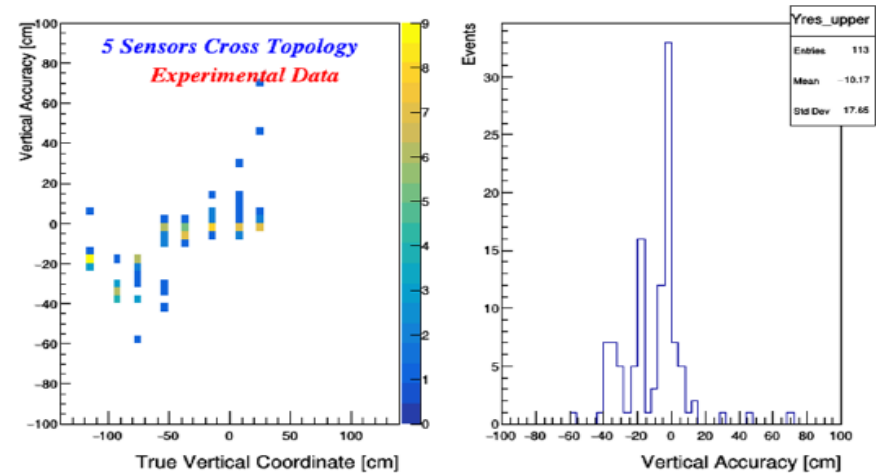
Experimental Results of unshielded ^{137}Cs Localization

Exposure time: 1 min,
Source Activity: $180\mu\text{Ci}$

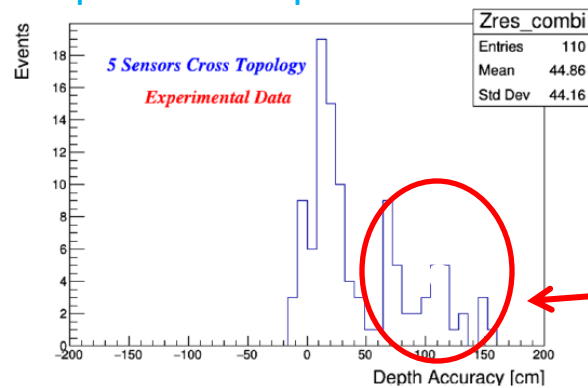
Horizontal source position resolution



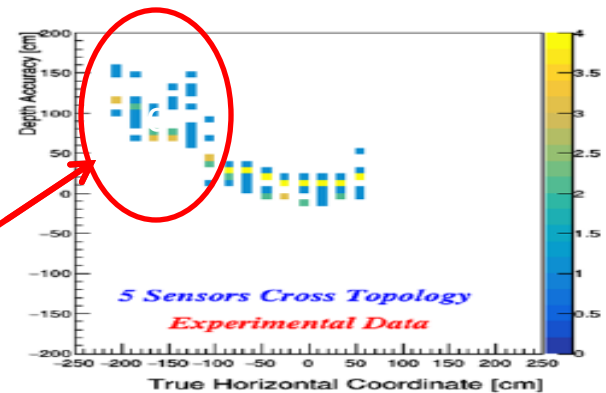
Vertical source position resolution



Depth source position resolution



Poor Depth localization when at edges

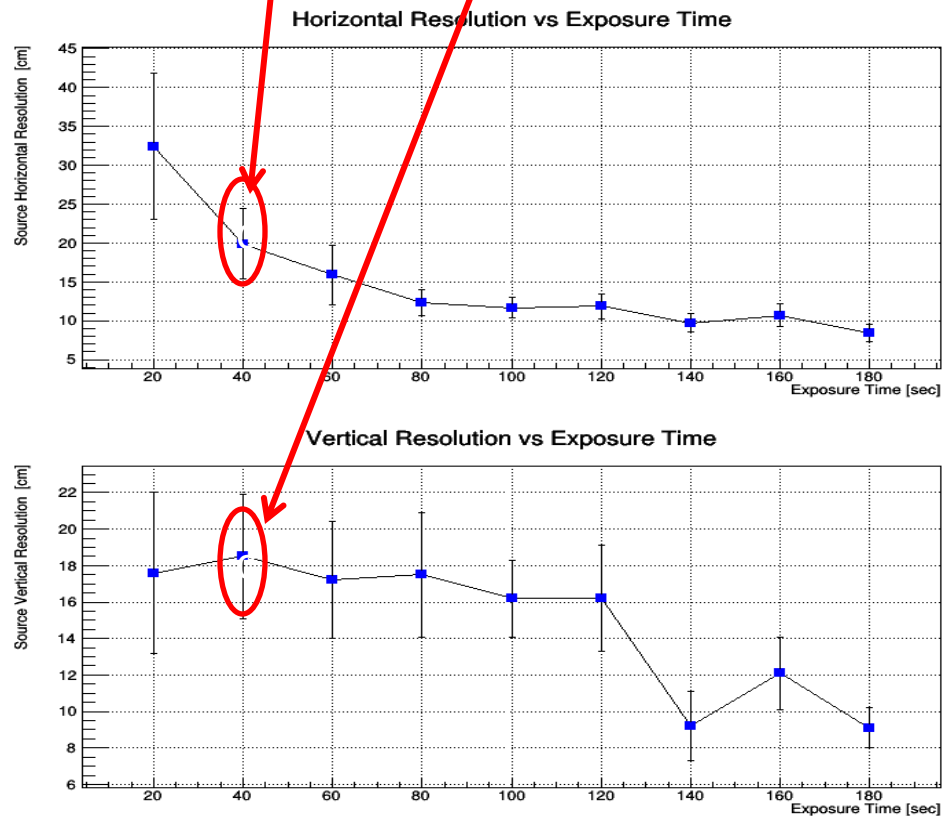


Experimental Results of light shielded ^{137}Cs Localization

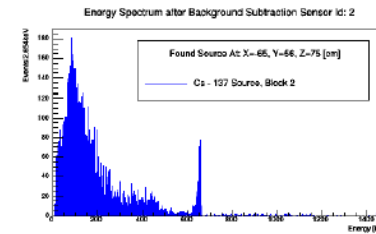
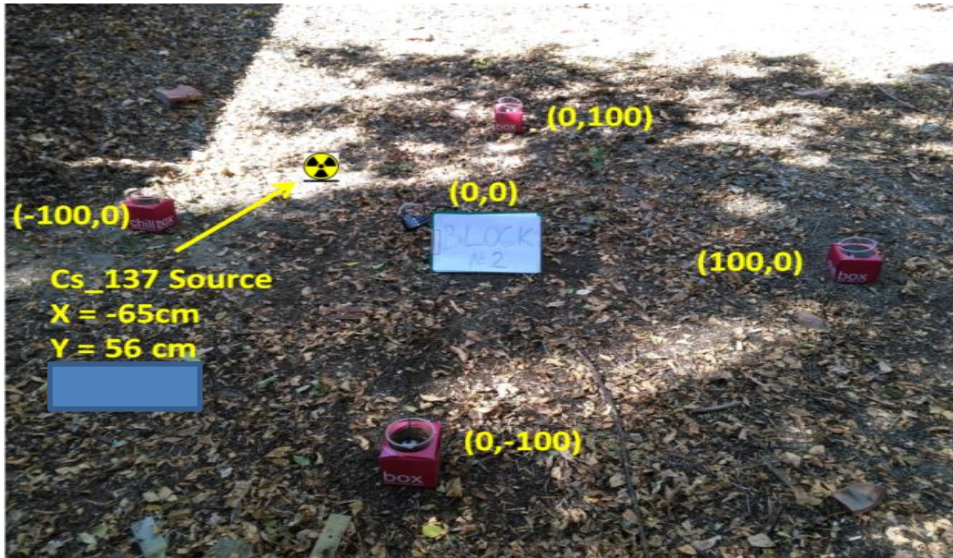
1cm Pb shield around an ^{137}Cs source of activity $180\mu\text{Ci}$



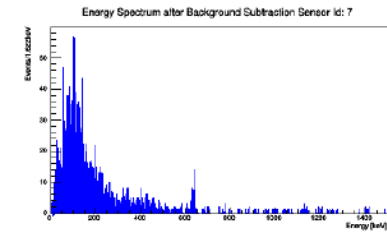
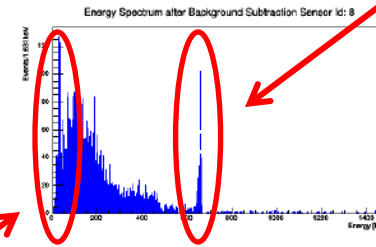
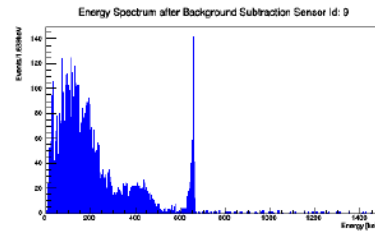
Both Horizontal and Vertical Resolution < 20cm in 40sec of exposure



Open Field Results in Sofia, Bulgaria(I)

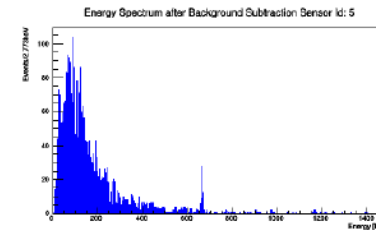


γ -ray : 662keV

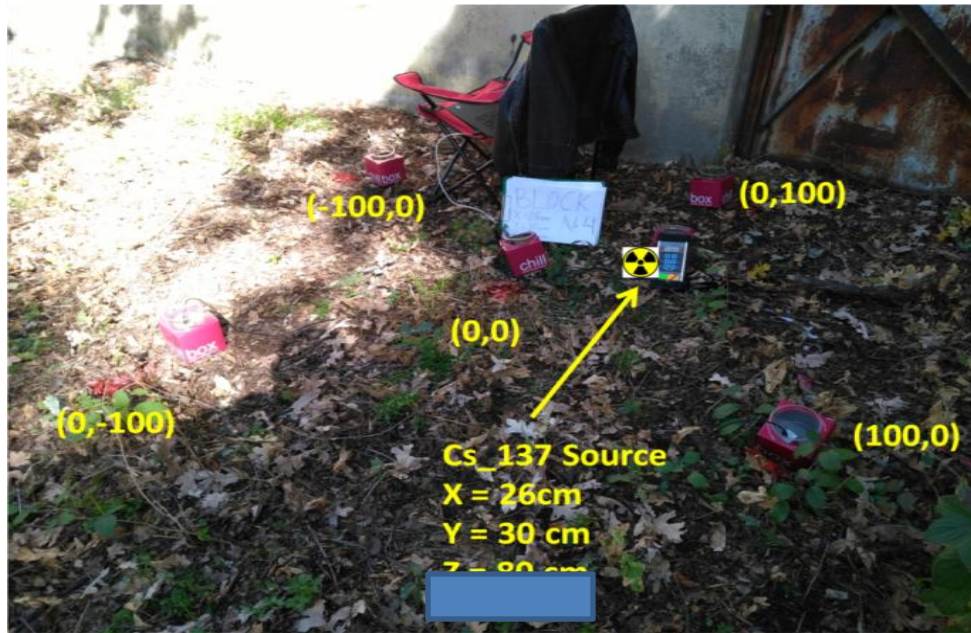


Not Known Surface Contamination of ^{137}Cs type

X-ray : 32keV



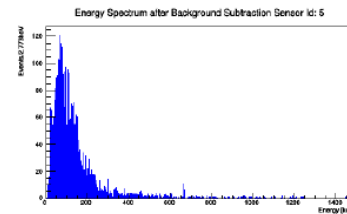
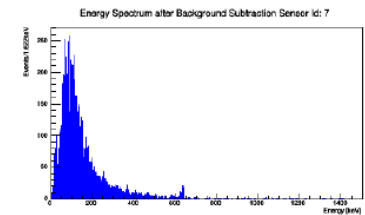
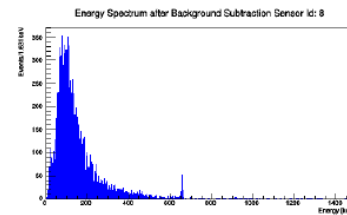
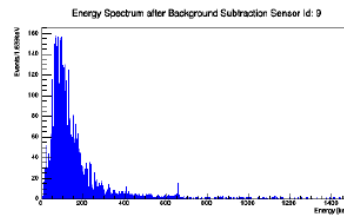
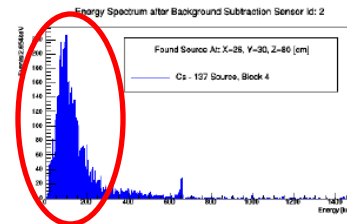
Open Field Results in Sofia, Bulgaria(II)



Scattered Spectrum



Not Known
Buried
Contaminat
ion of ¹³⁷Cs
type





A 2-D localization of a lightly shielded radiation source using a network of small form factor CZT sensors

G. Fragkos^a, K. Karafasoulis^b, A. Kyriakis^c, C. Potiriadis^d

^aHellenic Army General Staff R&IT Directorate (HAGS/R&IT Dir), ^bHellenic Army Academy, Vari, Attiki, 16673 Greece, ^cInstitute of Nuclear and Particle Physics, NCSR "DEMOKRITOS" Agia Paraskevi- Attiki, 15341 Greece, ^dGreek Atomic Energy Commission, Agia Paraskevi- Attiki, 15341 Greece
Email : kyriakis@inp.demokritos.gr



INTRODUCTION

Illicit trafficking of radioactive substances and the risk of their use in radiological bombs (dirty bombs) is a problem that the research community has been experiencing in recent years. Their localization is particularly difficult and from time to time a variety of detection methods have been proposed, particularly in areas with relatively defined inputs / outputs e.g. in ports and airports. However, their identification in open spaces e.g. squares, stadiums have a greater degree of difficulty. Below is a method of detecting radioactive substances in open spaces, which was studied by our team.

DETECTION APPARATUS

We used solid-state CZT spectroscopic detectors, of the type shown in Figure 1 below. These detectors are of small size but very sensitive and record the energy spectrum of the radiation emitted by radioactive materials (X, γ radiation).



Figure 1: Solid state spectroscopic CZT detectors.

A system of five such detectors in cruciform topology (Figure 2) records the gamma-ray spectrum in real time. The data are transmitted to a central computer station for processing. A ¹³⁷Cs radiation gel source of about 7MBq embedded in a Pb cylinder of 1cm width was used to test the performance of the source localization algorithms.

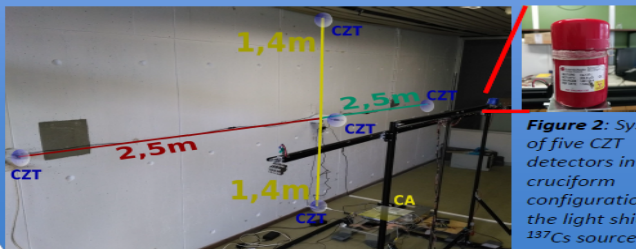


Figure 2: System of five CZT detectors in cruciform configuration and the light shielded ¹³⁷Cs source.

SPECTRAL RESPONSE

The spectral response of the system for a ¹³⁷Cs light shielded radioactive source located in an arbitrary point inside a monitoring area of 500 × 280 × 200 cm³ is shown in Figure 3.

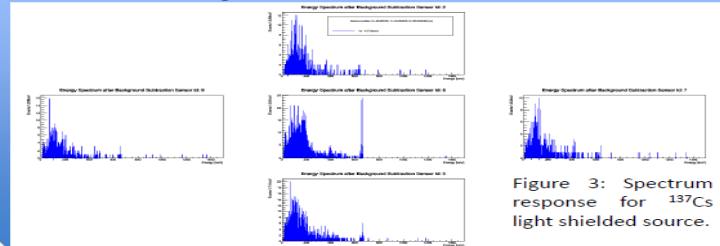


Figure 3: Spectrum response for ¹³⁷Cs light shielded source.

ALGORITHMS - SYSTEM RESPONSE

After processing the spectra in the central computing station using analytical algorithms and machine learning techniques, the location of the radioactive material can be estimated with a resolution better than 20 cm in horizontal and vertical directions for an exposure time of at least 40sec (Figure 4).

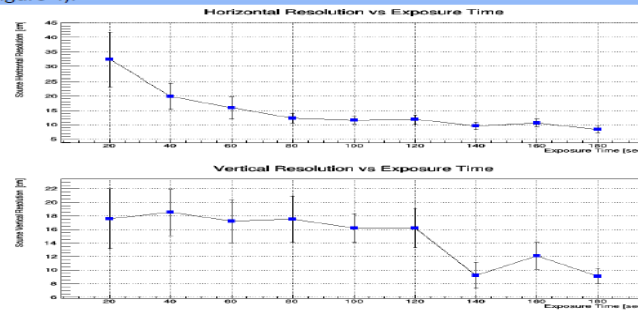


Figure 4: Horizontal (up) and vertical (down) position resolution of the light shielded ¹³⁷Cs radioactive source.

CONCLUSIONS

A network of five small form factor solid state CZT detectors in cruciform topology was used for a 2-D localization of lightly shielded radiation sources. Both analytical algorithms and machine learning techniques, show that the location of the radioactive material can be estimated with a resolution better than 20 cm in horizontal and vertical directions for an exposure time of at least 40sec.

This work was financially supported by NATO Sfp-984705

Conclusions for Radioactive Source Localization

- Results to localize both unshielded and light shielded Radioactive sources using Analytic and MVA algorithms are very promising.
- The full system was developed and can be used also in outdoor measurements.
- The gained knowhow is significant.

Carbon Nanotube Schottky type UV Sensor

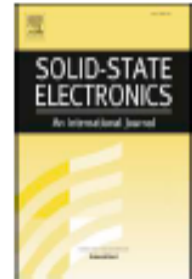
Solid State Electronics 151 (2019) 27–35



Contents lists available at ScienceDirect

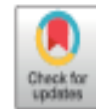
Solid State Electronics

journal homepage: www.elsevier.com/locate/sse



Carbon nanotube Schottky type photodetectors for UV applications

A. Filatzikioti^a, N. Glezos^b, V. Kantarelou^c, A. Kyriakis^c, G. Pilatos^b, G. Romanos^b, T. Speliotis^b,
D.J. Stathopoulou^a



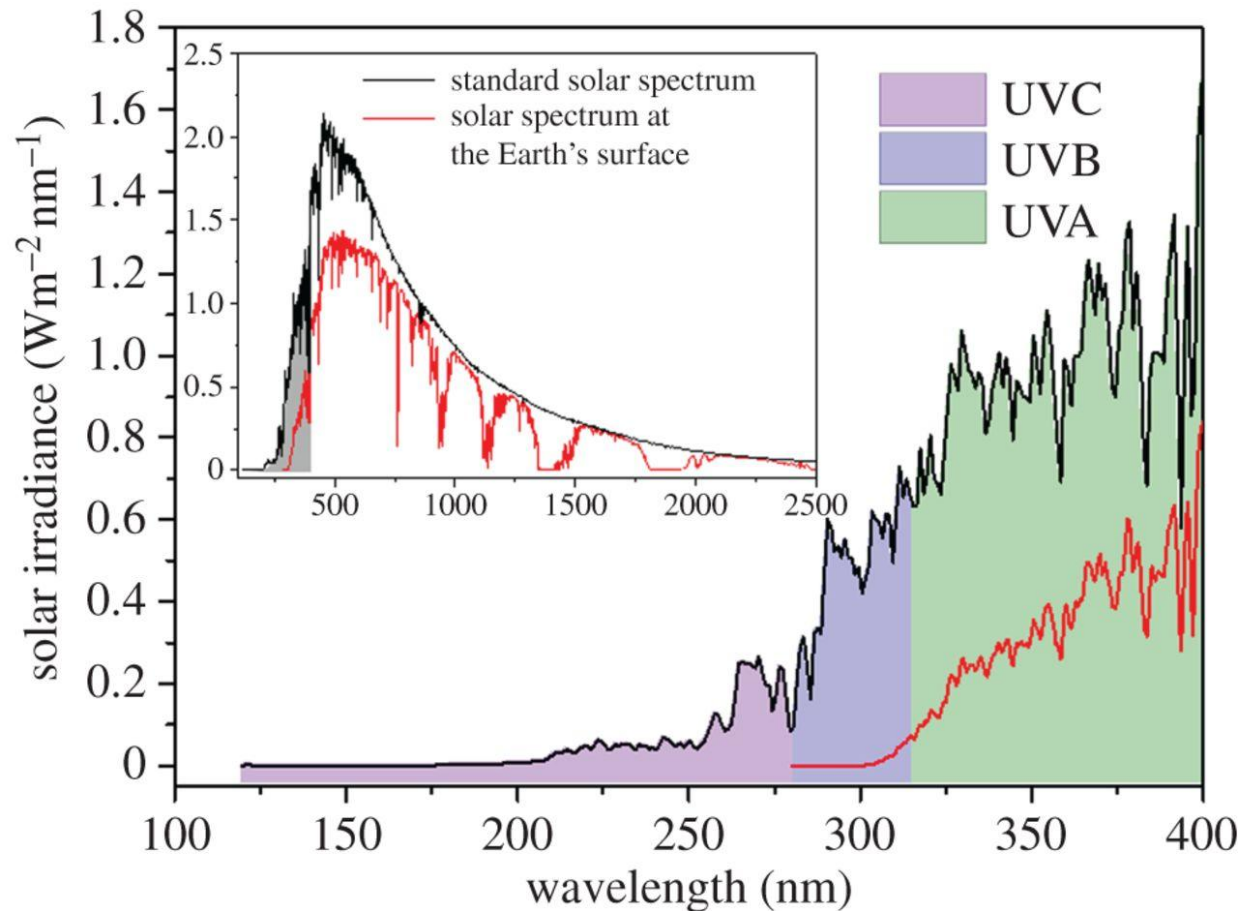
^a National Technical University of Athens, Iroon Polytechniou 9, 157 80 Athens, Greece

^b Institute of Nanoscience and Nanotechnology, NCSR Demokritos, Aghia Paraskevi, Athens 15310, Greece

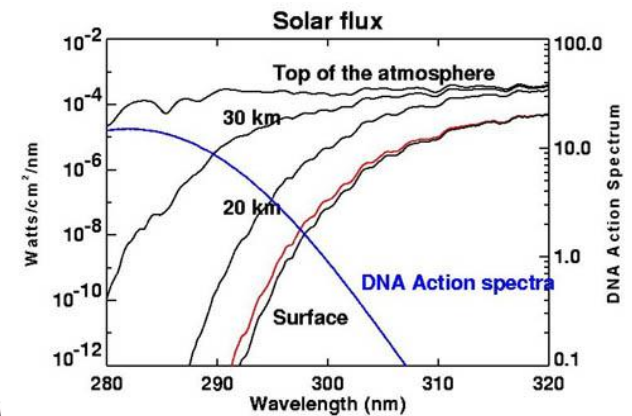
^c Institute of Nuclear and Particle Physics, NCSR Demokritos, Aghia Paraskevi, Athens 15310, Greece

<https://doi.org/10.1016/j.sse.2018.10.018>

Solar Spectrum



UV reduction caused by the ozone layer 20 and 40 Km above earth's surface.

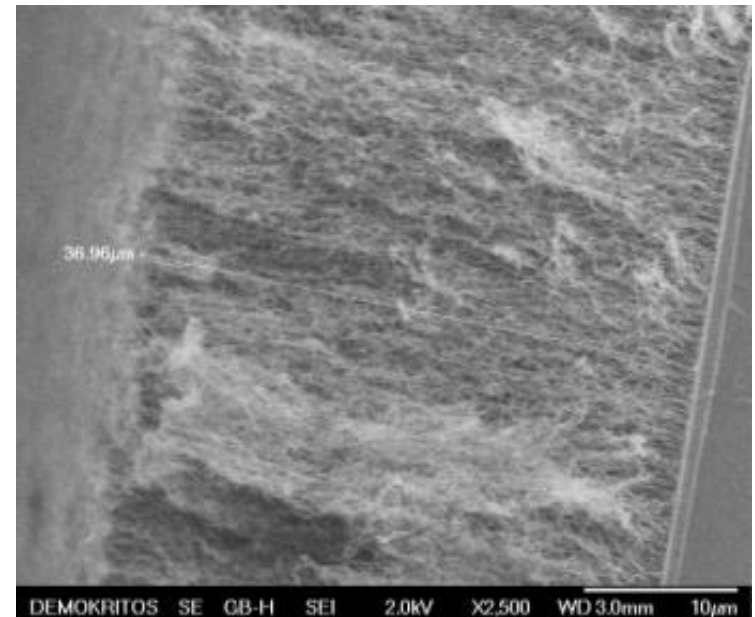
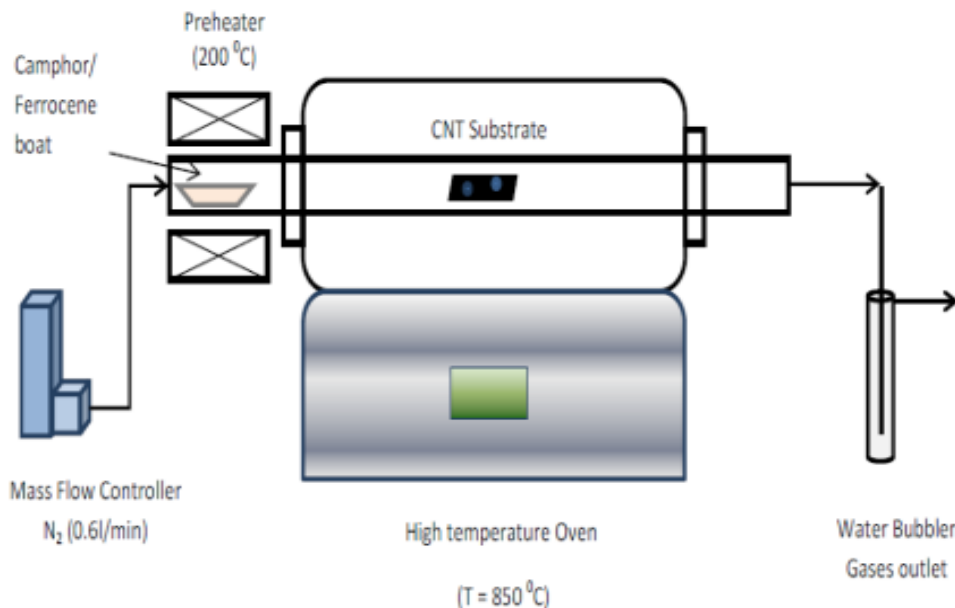


Introduction-Main Idea

- Many types of Ultra Violet (UV) detectors are used up to now.
- UV spectrum is of particular interest not only in particle physics where Cherenkov light and scintillators emit in this region but also in other fields like agriculture, food industry or medicine.
- The main idea is to build low cost and low operating voltage UV, sensors based on arrays of well-aligned Carbon Nano Tubes (CNT) in the form of Multi Wall CNT (MWCNT)

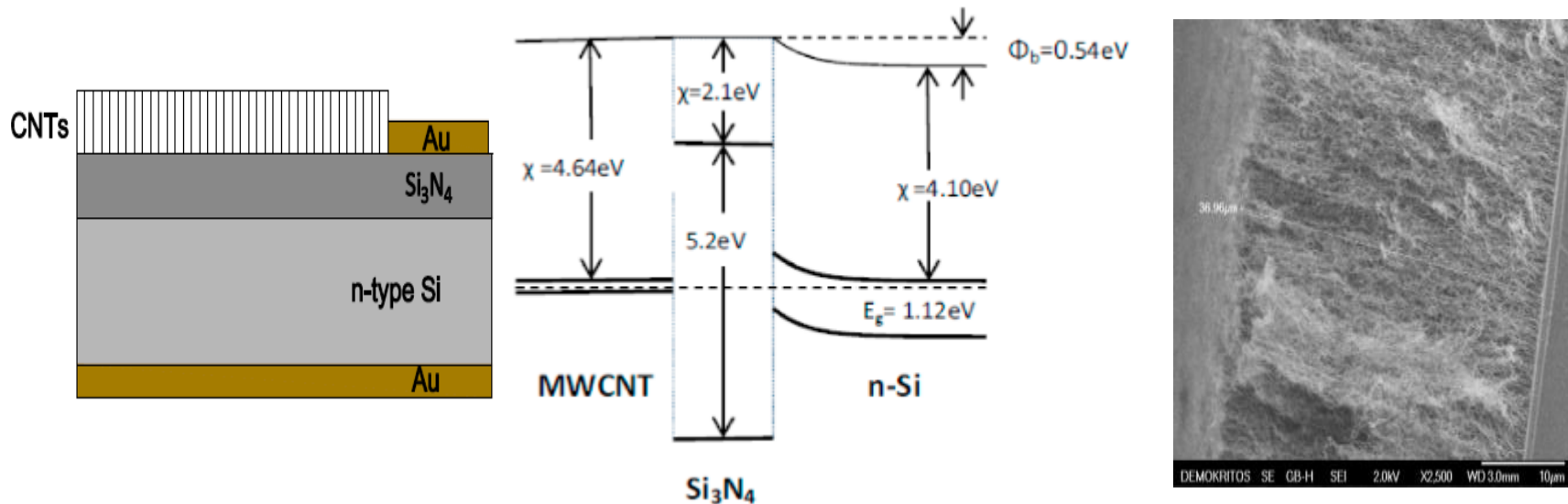
CNT Development Facility

- A mixture of 2g of Camphor with 0.1g of Ferrocene as a catalyst .
- Preheating phase at $T = 200\text{ }^{\circ}\text{C}$ and main high temperature oven at $T = 850\text{ }^{\circ}\text{C}$.
- The whole process lasts about 40min.
- Achieved to control the length in the CNT array below $40\mu\text{m}$.



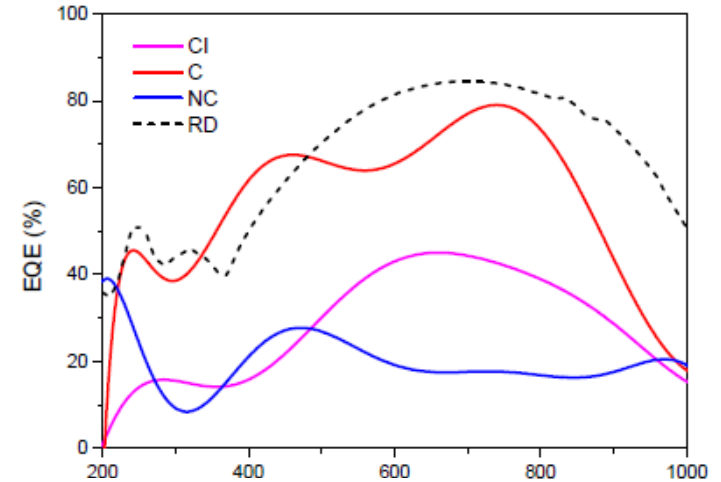
Sensor Fabrication

- n-type Si (450 μm width) of 100 orientation and $\rho = 10\Omega\cdot\text{cm}$.
- The back plain of the Si is covered with a thin layer (30 μm) of gold (Au) to serve as Ohmic contact.
- 140 μm Si_3N_4 layer is deposited on the top plain to serve as a diffusion barrier (i.e. Fe from Ferrocene during CNT development) as well as a dark current reducer.
- The CNTs were deposited using CVD process at 850 $^{\circ}\text{C}$

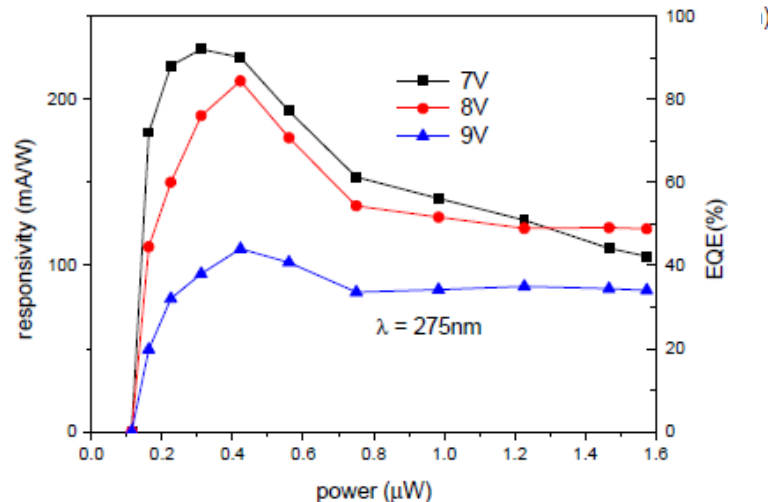


Sensor Performance

- Effective Quantum Efficiency (EQE) of the fabricated sensor for 9V bias voltage.
- Good performance in UV (200nm – 400nm).
- Peak EQE in IR (750nm).



- Responsivity /EQE as a function of the bias voltage and irradiation power from a LED emitting at $\lambda = 275\text{nm}$



Now funded by HFRI and GSRT program No 157446/12/21-9-2018, 200kEuro

A UV photodetector based on ordered free standing MWCNT

A. Kyriakis^a, N. Glezos^b, D. Velessiotis^b and A. Stefanou^c

^a Institute of Nuclear and Particle Physics, NCSR Demokritos, Aghia Paraskevi, Athens 15310, Greece, ^b Institute of Nanoscience and Nanotechnology, NCSR Demokritos, Aghia Paraskevi, Athens 15310, Greece, ^c National Technical University of Athens, Iroon Polytechniou 9, 157 80 Athens, Greece
E-mail: kyriakis@inp.demokritos.gr

Summary: Multiple Wall Carbon Nanotubes (MWCNT) present advantages for optoelectronic applications such as the large effective photo-collector surface as well as the possibility to tune their band gap and absorbance through the growth parameters[1]. In this work, we demonstrate a hybrid MWCNT/Si₃N₄/n-Si photodetector based on ordered MWCNTs and evaluate its performance in the UV, visual and near IR spectrum (200-1000nm). Depending on the application the absorbing nanotube layer can be made thick enough (e.g. several millimetres) to enhance radiation absorption and electron-hole pair generation. The best result obtained so far as a UV detector is a 90% Equivalent Quantum Efficiency @275nm for a 20µm CNT layer thickness[2].

Device Fabrication

The device structure is presented in figure 1. Fabrication starts with a n-type (100) Si wafer (450µm thickness) of $\rho = 10 \Omega \cdot \text{cm}$. The back plain of the Si is covered with a thin (100nm) of gold (Au) electrode, while a 150µm Si₃N₄ layer is deposited via Chemical Vapor Deposition (CVD) to serve as an anti-reflecting coating as well as a dark current reducer. This is followed by the development of the Carbon Nanotubes (CNT) layer via Catalytic CVD and the thermal evaporation of an aluminum (Al) thin (100nm) electrode.



Figure 1: Device Structure

The reactor used for the CNT development is displayed in figure 2. A mixture of 2g of Camphore with 0.1g of Ferrocene as a catalyst was injected into the deposition chamber with the use of N₂ gas flow (0.6l/min), after preheating at 200°C. The mixture gas travels through the main high temperature oven, which is kept at $\theta = 850^\circ\text{C}$ and MWCNTs are formed on the “cold” substrate. The whole process lasts about 40min and produces well-ordered MWCNTs (Figure 3).

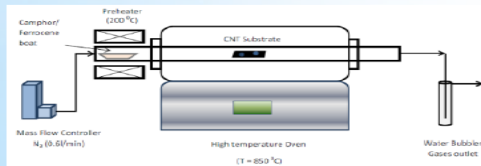
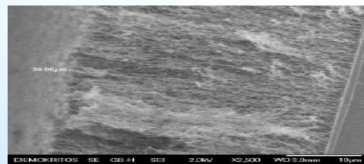


Figure 2: The CNT development facility with the High Temperature Oven

Figure 3: MWCNTs of 20µm length and 15nm diameter



Operation

When used as a photodetector, the device is biased in the inverse direction (n-Si substrate positive) and behaves as a Schottky diode with an intermediate dielectric barrier layer. Figure 4 shows the band scheme of the device. The Si₃N₄ layer acts as a wave guide for UV photons and as a diffusion barrier for the Fe ions introduced during MWCNT fabrication (Figure 5)

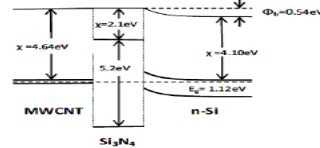
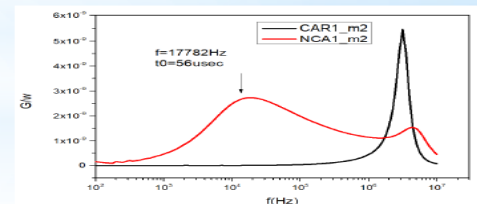


Figure 4: The MWCNT/Si₃N₄/Si heterojunction as it is considered as a Schottky diode (0.54eV barrier) with an intermediate dielectric layer carrying Fe traps.

Figure 5: The CNT formation procedure requires the presence of Fe catalyst. This is blocked by the Si₃N₄ layer resulting in donor/acceptor traps with a characteristic time of 56µsec.



Performance

The device has excellent performance in the UV and the visual part of the spectrum. Responsivity and EQE exceed 100mA/W and 50% for a selected operation bias. The UV response is shown in figure 6.

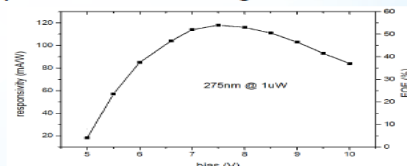


Figure 6: Responsivity and EQE for a 275nm source vs device bias [2]

References

- [1] C. Aramo *et al.*, “Progress in the realization of a silicon-CNT photodetector,” *Nucl. Inst.*
- [2] A. Filatzikioti *et al.*, “Carbon nanotube Schottky type photodetectors for UV applications,” *Solid. State. Electron.*, vol. 151, pp. 27-35, 2019.

Conclusions for CNT UV Sensors

- We developed CNT sensors that can operate:
 - In a wide range of the UV spectrum (200nm – 400nm)
 - Have large responsivity $\sim 200 \text{ mA/W}$ for UVC band
 - They can operate in low voltage $< 10 \text{ V}$.
 - The development process and production is cheap.
 - They are promising UV radiation sensors

Supervised Theses

- “FCNC top decays in CMS/LHC”, Grigoris Vermisoglou, Athens 2007, <http://hdl.handle.net/10442/hedi/20088>
- “aTGC Studies in $Z\gamma$ channel in CM/LHC”, Eleni Petrakou, Athens 2011, <http://hdl.handle.net/10442/hedi/27701>, DOI: [10.12681/eadd/27701](https://doi.org/10.12681/eadd/27701)
- “Search for New Physics in final states with photons and missing transverse energy, with the CMS experiment, at CERN”, Iasonas Topsis-Giotis, Athens 2017, <http://hdl.handle.net/10442/hedi/41402>
- “Search for SUSY in T5gg and T6gg Models in CMS/LHC”, Garifallia Paspalaki, in progress

Reviewer

IEEE Transactions on Nuclear Science
(TNS)

Conferences Organization

ERDIT 2016, Athens, <https://indico.cern.ch/event/464127/>



ERDIT in Athens

11-12 April 2016
Demokritos, ATHENS
Europe/Athens timezone

Search... 

Overview

Scientific Programme

Timetable

Contribution List

My Conference

My Contributions

Registration

Participant List

Meeting directions:<http://www.demokritos.gr/Contents.aspx?CatId=28>

This is the 6th meeting of the European Radiation Detectors and Imaging Technology Network, **ERDIT** (www.erdit.eu). The meeting will discuss the latest European funding progress on radiation detectors and imaging technology with particular attention to future openings. The meeting will start with a short course on radiation detectors for students and young researchers on Monday morning.

A discussion on "How to write a successful grant proposal for H2020" will also be part of the programme together with a presentation on the latest developments of **ATTRACT**, a new, open, pan-EU initiative to accelerate the development of high-performance detector and imaging technologies for market - through a process of co-innovation among European research institutes, small and medium enterprises (SMEs), companies and universities. (<http://www.attract-eu.org/>).

The meeting will be held in the National Center Of Scientific Research (N.C.S.R.) "**Demokritos**" (<http://www.demokritos.gr/default.aspx?lang=en>), located about 30 minutes by metro & Bus from Athens city centre. Athens International Airport is located 20Km away - <http://www.demokritos.gr/Contents.aspx?CatId=28> from the meeting venue. The Center Of Scientific Research (N.C.S.R.) "Demokritos" is the biggest Multi-disciplinary Research Centre in Athens.

iWoRiD 2019, Crete, <https://indico.cern.ch/event/774201/>



21st International Workshop on Radiation Imaging Detectors

7-12 July 2019

- Welcome to iWoRiD 2019
- Programme
 - ↳ Presentation Guidelines
 - ↳ Proceedings
- Timetable
- Call for Abstracts
- My Conference
 - ↳ My Contributions
- Registration
- Registration information
- Committees
- Exhibition
- Book of Abstracts
- Participant List
- Venue
 - ↳ Travel to Kolympari, Chania, Crete, Greece
 - ↳ Conference Venue
 - ↳ Accommodation
 - ↳ Social Events
 - ↳ Practical information
- Industrial exhibition

Welcome to iWoRiD 2019

The International Workshop on Radiation Imaging Detectors are held yearly and provide an international forum for discussing current research and developments in the area of position sensitive detectors for radiation imaging, including semiconductor, gas and scintillator-based detectors. Topics include processing and characterization of detector materials, hybridization and interconnect technologies, design of counting or integrating electronics, readout and data acquisition systems, and applications in various scientific and industrial fields. The workshop will have plenary sessions with invited and contributed papers presented orally and in poster sessions. The invited talks will be chosen to review recent advances in different areas covered in the workshop.

This year the Workshop will be arranged for the 21st time on July 7-12, 2019 in Kolympari, Chania, Crete, Greece, Welcome!

ATTENTION: The Abstract Submission Deadline has been extended to the 16th of April 2019.

iWoRiD 2019, Crete, <https://indico.cern.ch/event/774201/>



Future Plans

CMS/LHC Analysis

ELIDEK Phase II (Under Evaluation)

Title of proposal: *Development of the Phase II Silicon Tracker and Physics in the CMS Experiment at CERN*

Acronym: *DETRA*

Scientific Area: *Natural Sciences*

Scientific field/s: *Particles and Fields*

Principal Investigator (PI): *Dimitrios LOUKAS*

Host Organization: *NCSR DEMOKRITOS*

Proposal category: *III a*

- Search for general gauge mediated supersymmetry in events with photons, jets, and missing transverse momentum at 13 TeV center of mass energy in CMS/LHC experiment

CMS/HL-LHC

- Continue the IV, CV measurements of the structures (MOS, Diodes, Mini 2S) contained into the 2S wafer and check their response after heavy irradiation (up to 10Mrads → 100kGy) using ^{60}Co found in NCSR “Demokritos”.
- Try to setup a radiation model in TCAD in collaboration with the INFN Perugia.
- Contribute to all the work related to the main tasks of our lab (selected as Process Quality Control – PQC center) for the Tracker HL-LHC project.
- Study of HVCMOS technology for the development of monolithic CMOS sensors (work will be supported by ELIDEK program)
- Try to investigate new types of signal extraction for silicon sensors using Mach-Zehnder interferometers in collaboration with CERN

HV – CMOS Technology

An evolution of the MAPS concept:

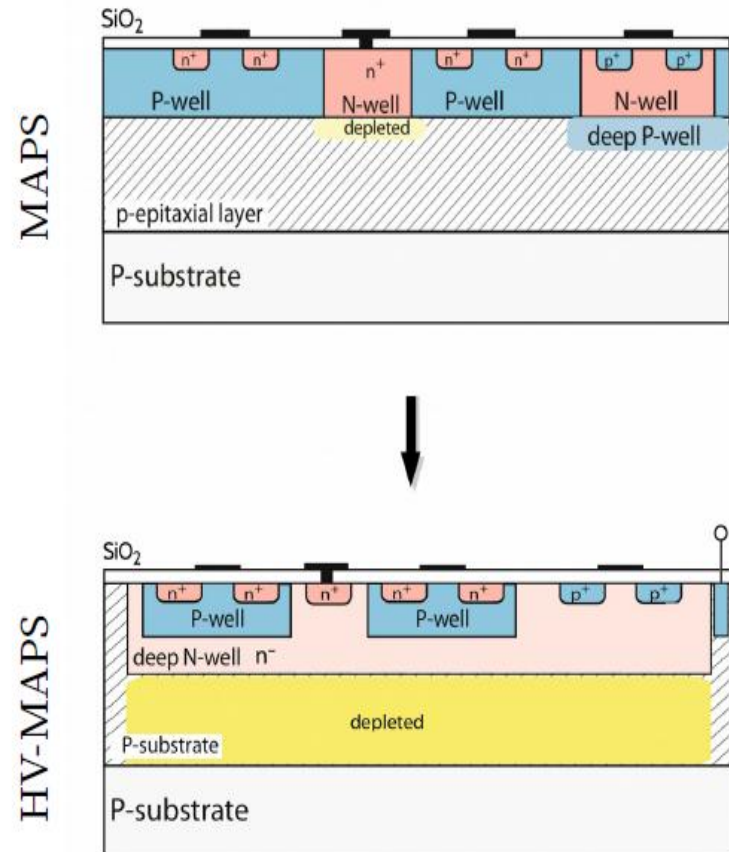
- integrate transistors into diode (“smart diode”, full fill factor)
- deep N-well shields low voltage devices
- HV required (based on HV-CMOS)
- fully or partially depleted sensor
- full CMOS

Main advantages:

- Epi layer fully depleted: charge collection by drift
- Collection time ~ 1 ns

[1] <https://arxiv.org/abs/1811.07817>

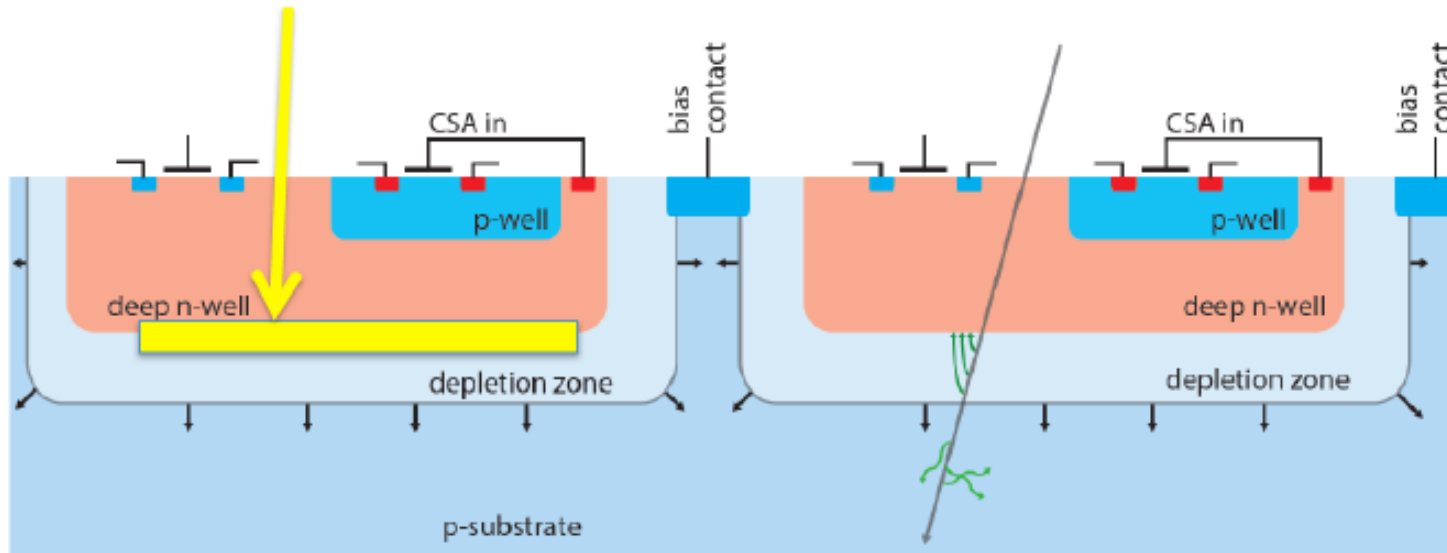
[2] <https://arxiv.org/pdf/1611.02669>



Christof Sauer

Fast-timing HV-CMOS?

Add a boron layer similar to LGAD



The HV-CMOS structure could be in principle modified to insert an avalanche layer to increase the timing performance, as in the LGAD detectors.

Low Gain Avalanche *Detectors* (LGAD) → fast response down to 30psec

<https://doi.org/10.1016/j.nima.2018.08.041>

CMS/HL-LHC – PHOTONICS

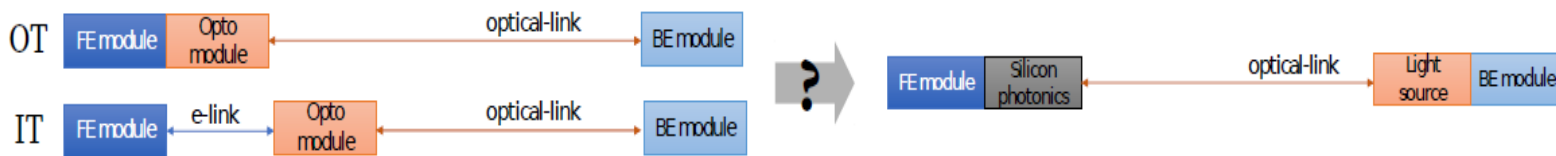
The issue:

- placing optical links on the detector crucial to reduce material
- not for Inner Tracker, because of lack of space and radiation tolerance of current technology

These limitations could be overcome by the use of Silicon Photonics, integrating the optical link directly into the front-ends.

Principle:

- Silicon is transparent in 1.3 – 1.6 μm
- Modulators can be built as reverse-biased pn junctions
- Advantages:
 - Radiation resistance potentially as good as Si-sensors and CMOS electronics
 - Possibility of co-integration with readout electronics: **less material in links**
 - Detector only modulates light, with the light source far from radiation: **less power/material**



Combine our UV sensor to a SiPM

Very challenging since we have to combine standard lithographic technology with MWCNT development process

Two ideas should be checked:

- Develop MWCNT in one top surface of a very thin Si layer ($\sim 100\text{-}150\ \mu\text{m}$) and develop the SiPM on the back side.
- Use MWCNT in solution instead and modify the process of SiPM by adding an extra Si₃N₄ layer on top to host the MWCNT solution.

Also:

- Investigate the possibility to develop a camera using CNT pixels of $0.5 \times 0.5\ \text{mm}^2$. We have already achieved CNT pixels of $1 \times 1\ \text{mm}^2$

KETEK GmbH (<https://www.ketek.net/>) has shown some interest to collaborate

Contribution to CORONA Horizon2020 project



CORONA – Effective uninterrupted safety inspection of border crossing cargo

Topic: BES-02-2019 (Sub-topic 4) – Technologies to enhance border and external security
(Detecting threats in the stream of commerce without disrupting business)

#	Participant organization name	Acronym	Country	Type
1	Institute of Communication and Computer Systems (Coordinator)	ICCS	GR	RTO
2	Thales SA	THA	FR	IND
3	EMC Information Systems International (DELL)	DELL	IR	IND
4	EtraInvestigacion Y Desarrollo SA	ETRA	ES	IND
5	SIVECO Romania S.A.	SIV	RO	IND
6	National Center for Scientific Research "DEMOKRITOS"	NCSR	GR	RTO
7	INOVA INESC Inovação – Instituto de Novas Tecnologias	INOV	PT	RTO
8	Maastricht University	MU	NL	ACA
9	University of Newcastle	UNEW	UK	ACA
10	Catalink Ltd	CTL	CY	SME
11	Up2Metric	U2M	GR	SME
12	IBATECH Tecnologia SL	IBA	ES	SME
13	Quantos Lux	QULUX	LU	SME
14	Administration of the State Border Guard Service of Ukraine	ASBGS	UA	LEA ¹
15	Ministry of Public Security - Israel National Police	MOPS-INP	IL	LEA ¹
16	MinistarstvounutrašnjihposlovaRepublikeSrbije	MOI	SB	LEA ¹
17	Inspectoratul Teritorial al Politiei de Frontiera Timisoara	ITPF	RO	LEA ¹
18	Valencia Local Police	PLV	ES	LEA
19	Valencia Port Foundation	VPF	ES	End User
20	Thessaloniki Port Authority	THPA	GR	End User
21	Piraeus Port Authority	PPA	GR	End User
22	Trieste Port Authority	TPA	IT	End User
23	SC TransferoviarGrup SA	TFG	RO	End User

Contribution to:

“ΕΡΕΥΝΩ – ΔΗΜΙΟΥΡΓΩ – ΚΑΙΝΟΤΟΜΩ “ (Β’ Κύκλος)

→ Συμπράξεις Επιχειρήσεων με Ερευνητικούς Οργανισμούς

Proposal Title:

Development of a smart system with artificial intelligence, safe bio-markers and broadband sensors and infrared cameras for an efficient surgery process for ovarian cancer.

- NCSR “DEMOKRITOS”, 4/5 Institutes
- “ALEXANDRA” Hospital
- MILTECK S.A.

THANK YOU